Control law adaptation for helicopter in turbulent air

Qi Lin

Thesis to obtain the Master of Science Degree in

Aerospace Engineering

Supervisor: Prof. José Raúl Carreira Azinheira

Examination Committee

Chairperson:	Prof. João Manuel Lage de Miranda Lemos
Supervisor:	Prof. José Raúl Carreira Azinheira
Members of the Committee:	Prof. Filipe Szolnoky Ramos Pinto Cunha

November 2015

Acknowledgments

This work would not have been possible without the contributions and support of the kind people around me.

I would like to thank all the PGV department of Thales Avionics for this great opportunity and wonderful experience. I would like to thank Romain for his technical advice and orientation during all my internship. I thank Clément, Dominique, Foucauld, Julien, Luis, Natacha, Thomas and Vicente for the great time we spend together during this internship.

I also thank Joel Gomes for his unceasing encouragement, support and attention every day. Last but not the least, I would like to thank all my friends and family, for supporting me spiritually throughout my life.

Resumo

Actualmente, o *Automatic Flight Control System* (AFCS) é utilizado para ajudar o piloto a realizar as suas tarefas, a fim de reduzir sua carga física e cognitiva. No entanto, o ajuste do AFCS normalmente é um compromisso entre desempenho e conforto.

Neste estudo, um exemplo de AFCS do helicóptero é considerado. O objectivo deste estágio na Thales Avionics é modificar este AFCS para aumentar o conforto de passageiros em ar turbulento, mantendo um bom desempenho em ar calmo.

A metodologia seguida é a concepção de um mecanismo de detecção de turbulência, que deve ser capaz de seleccionar o controlador original em ar calmo, e em caso de detecção de turbulência, mudar o controlador para aquele que aumenta o conforto.

A fim de aumentar o conforto dos passageiros em ar turbulento, a actividade do AFCS é reduzida para eliminar as acelerações indesejáveis sentidas pelo helicóptero. Este estudo foi centrado no sistema de controlo de velocidade, e as modificações realizadas sobre este sistema pretendem minimizar a aceleração longitudinal encontrada em ar turbulento.

Os resultados obtidos são quantificados utilizando o padrão de avaliação de conforto dos passageiros (ISO-2631).

Palavras-chave: *Automatic Flight Control System*, conforto, desempenho, ar turbulento, helicóptero, mecanismo de detecção de turbulência

Abstract

Nowadays, Automatic Flight Control System (AFCS) is used to assist the pilot in performing his tasks in order to reduce his physical as well as cognitive load. However, tuning the AFCS is usually a compromise between performance and comfort.

In this study, an example AFCS of helicopter is considered. The goal of this internship in Thales Avionics is to modify this AFCS to improve passengers comfort in turbulent air, while keeping good performance in calm air.

The followed methodology is to design a turbulence detection mechanism, which is able to select the original tuning in calm air, and in case of turbulence detection, it switches the controller to the one that increases comfort.

In order to increase passengers comfort in turbulent air, the control activity of the AFCS is reduced to eliminate the undesired accelerations experienced by the helicopter. This study was focused on the speed control system, and the modifications performed on this system intend to minimize the longitudinal acceleration encountered in turbulent air.

The results obtained are quantified using standard passenger comfort evaluation methodologies (ISO-2631).

Keywords: Automatic Flight Control System (AFCS), comfort, performance, turbulent air, helicopter, turbulence detection mechanism

Contents

List of Symbols

Abbreviations

Abbreviation	Meaning
AP	Autopilot
AFCS	Automatic Flight Control System
ADU	Air Data Unit
AHRS	Attitude and heading reference system
APCP	Autopilot Control Panel
APPR	Approach mode
ALT	Altitude mode
ATT	Attitude retention system
AXBI	Filtered inertial acceleration
CAS	Calibrated Airspeed
CBT	Cyclic Beep Trim
FD	Flight Director
FTR	Force Trim Release
HDG	Heading mode
IAS	Indicated Airspeed
ISO	International Organization for Standardization
NAV	Navigation mode
PIP	Percentage of Ill Passengers
RMS	Root Mean Square
RPM	Revolution Per Minute
SAS	Stability Augmentation System
VDI	Association of German Engineers
VS	Vertical Speed mode
VXBI	Filtered airspeed

Latin Symbols

Symbols	Designation
a	Overall vibration
a_v	Total vibration value
$\bar{a_w}$	RMS of the frequency weighted acceleration
a_{wx}	RMS of the frequency weighted acceleration on x axis
a_{wy}	RMS of the frequency weighted acceleration on y axis
a_{wz}	RMS of the frequency weighted acceleration on z axis
f_{rms}	RMS of a continuous function
K_a	Velocity gain factor
K_b	Acceleration gain factor
K_θ	Pitch angle gain factor
K_q	Pitch rate gain factor
k_x	Weighting factor for x axis
k_y	Weighting factor for y axis
k_z	Weighting factor for z axis
q	Pitch rate
sV_{ac}	Derivative of actual airspeed
T	Computation period
V_a	Measured airspeed
V_{ac}	Actual airspeed
V_e	Difference between V_{ac} and V_{sel}
V_{error}	Velocity error
V_i	Longitudinal inertial velocity
V_{ref}	Airspeed reference
V_{sel}	Selected airspeed
$\dot{V}$	Difference between $\dot{V}_i$ and sV_{ac}
$\dot{V}_i$	Longitudinal inertial acceleration
W_k	Vertical acceleration weighting curve for vibrating comfort defined in ISO 2631-1 (1997)
W_d	Horizontal acceleration weighting curve for vibrating comfort defined in ISO 2631-1 (1997)
W_f	Vertical acceleration weighting curve for motion sickness defined in ISO 2631-1 (1997)
x_{rms}	RMS of a set of samples

Greek Symbols

Symbols	Designation
δ_t	Throttle command signal
θ	Pitch angle
ϕ	Roll angle
ψ	Yaw angle
θ_{ref}	Pitch angle reference
ϕ_{ref}	Roll angle reference
ψ_{ref}	Yaw angle reference

List of Figures

List of Tables

1 Introduction

The well being and comfort of passengers have always been a concern for the aerospace industry. During flight in calm air, aircraft are quite comfortable. However, in a turbulent air environment, where the movement of air mass changes suddenly in direction and intensity, aircraft are constantly experiencing positive and negative acceleration forces in different directions. Exposure to these accelerations may origin discomfort and interfere with pilots working activities during the flight.

Nowadays, pilots use an Automatic Flight Control System (AFCS) to reduce their workload, improve mission reliability and enhance safety of flight. However, tuning an AFCS is a compromise between performance and comfort. On the one hand, it is important to achieve desired performance in calm air; on the other hand, it is desired to have a comfortable flight in a turbulent environment.

The base tuning of the AFCS considered in this study is biased towards performance. The goal of this internship in Thales Avionics is to modify this AFCS in order to increase passengers comfort in turbulent air, while providing good performance in calm air.

1.1 Thesis outline

Apart from introduction and conclusion, the present thesis is divided in 6 chapters.

Helicopter basics are described in chapter 2. Helicopter AFCS is presented in chapter 3, where its components and operations are portrayed. Chapter 4 exposes the internship context. Chapter 5 is dedicated to the results of bibliographic research. The first part is related to the existing control law for rejecting turbulence disturbances, where contents of two papers from US patent are presented. The second part describes a comfort evaluation method based on the international ISO 2631 standard, which may allow us to evaluate the improvements of the new control law. The modifications on the AFCS concerning the control activity reduction and turbulence detection mechanism, as well as the obtained results are discussed in the chapter 6. Finally, chapter 7 contains the evaluation with flight test data.

For reasons of confidentiality, numerical values of figures are omitted, therefore, a qualitative evaluation of the results are presented.

2 Helicopter basics

2.1 Helicopter lift

Aircraft are able to fly due to lift generated by the effect of airflow as it passes around an airfoil. When the airflow encounters an airfoil, the flow is split over and under the airfoil and, it generates aerodynamic force. This force is normally resolved into two components, lift and drag. The lift is the force component perpendicular to the airflow direction and the drag is the component parallel to the direction of the airflow, as shown in figure 2.1.

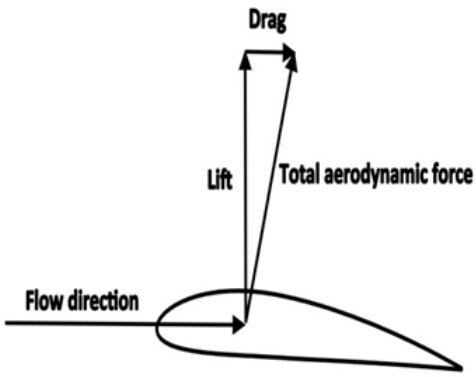

Figure 2.1: Aerodynamic force generated by an airfoil

The rotor blades of helicopters are built with airfoil-shaped cross sections, and its rotation around the mast forces the air to pass around them and, hence generates an aerodynamic force. The lift component generated by airfoils depends on the speed of the airflow, density of the air, shape of the airfoil, and angle of attack between the air and the airfoil. Therefore, one can increase the lift of helicopter by increasing the rotor rotation to augment the airspeed. However, this solution is not used because the rotation speed of the rotor is maintained constant during the flight. The other way to increase the lift is to increase the angle of attack by increasing the angle of incidence of the rotor blades.

The angle of attack should not be confused with the angle of incidence. The angle of attack is the angle between the airfoil chord line and the resultant relative wind, while the angle of incidence is the angle between the chord line and the reference plane containing the rotor hub (tip-path plane). Angle of incidence and angle of attack are exposed respectively in figure 2.2 and figure 2.3. The angle of incidence is a mechanical angle rather than an aerodynamic angle and is sometimes referred to as blade pitch angle. Pilots are able to adjust the pitch angle by moving the flight controls. A change in the pitch angle results into a change in angle of attack. If the pitch angle is increased, the angle of attack is increased, if the pitch angle is reduced, the angle of attack is reduced. It is known that a change in the angle of attack

changes the coefficient of lift, which changes the lift created by the airfoil. Therefore, pilots can use flight controls to change the blade pitch angle in order to modify the lift.

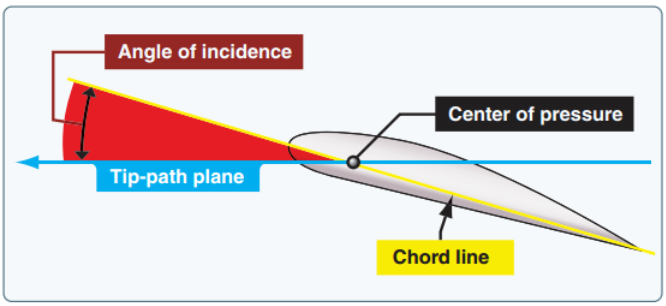

Figure 2.2: Angle of incidence [1]

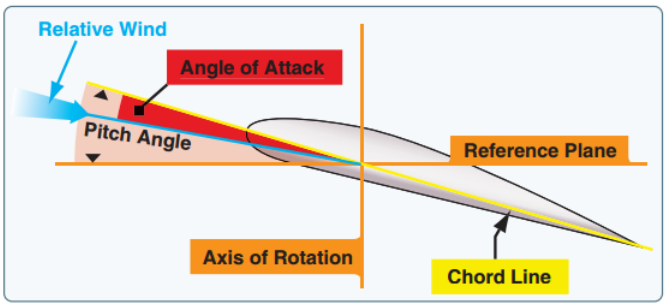

Figure 2.3: Angle of attack [1]

The overall lift, provided by the rotor blades, is called the total lift-thrust force or total rotor thrust and it acts always perpendicular to the tip-path plane or rotation plane of the main rotor. The tip-path plane is the imaginary plane made by the tips of the blades (see figure 2.4). During hovering flight in a no-wind condition, the tip-path plane is horizontal and the total lift-thrust force acts straight up, as presented in figure 2.4. For a helicopter to hover, the total lift-thrust force must compensate the weight and drag forces which are acting straight down. Figure 2.5 shows the forces acting on the helicopter during hovering flight in a no-wind condition.

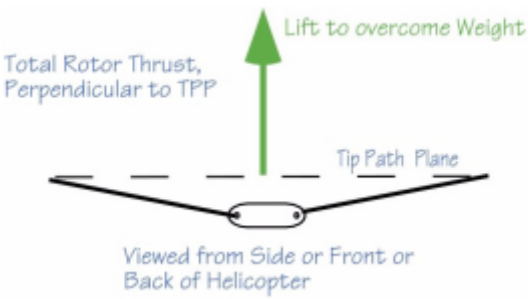

Figure 2.4: Horizontal tip path plane [2]

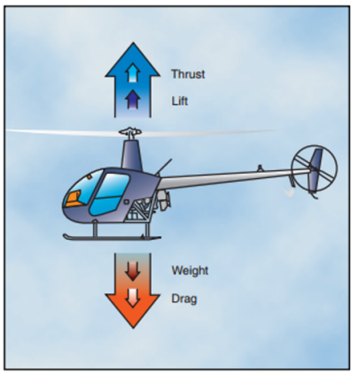

Figure 2.5: Thrust and lift compensates weight and drag during hovering flight in a no-wind condition [3].

When the tip path plane is tilt away from the horizontal, the total lift-thrust force can be divided into two components, the horizontal acting force, thrust and the upward acting force, lift. For example, in a transition from hover flight to forward flight, the tip path plane is tilted forward (figure 2.6), which tilts the total lift-thrust force forward from the vertical. The component thrust acts horizontally to overcome the drag and enables the helicopter to move forward. The forces components acting on the helicopter during forward flight can be observed in figure 2.7. Thanks to the capacity of tilting the rotor plane in any direction, the helicopter can move in any direction and perform hover flight in the presence of wind.

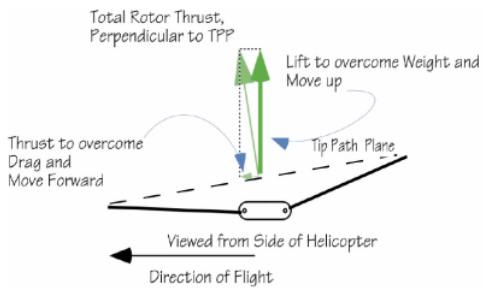

Figure 2.6: Tilted tip path plane in forward flight [2]

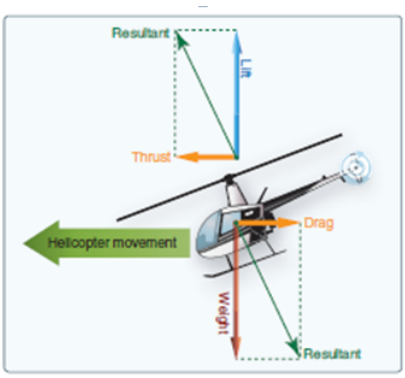

Figure 2.7: Forces acting on the helicopter during forward flight [1]

2.2 Gyroscopic precession

The spinning main rotor of a helicopter acts like a gyroscope. Due to gyroscopic precession, any force applied to a rotating body takes effect over 90 degrees later in the direction of rotation from where the force was applied. Figure 2.8 illustrates effects of precession on a typical rotor disk when force is applied at a given point. A downward force applied to the disk at point A results in a maximum downward movement of the disk at point B. Aircraft designers take gyroscopic precession into consideration and rig the cyclic pitch control system to create an input 90 degrees ahead of the desired action. Figure 2.9 shows reactions to forces applied to a spinning rotor disk by control input.

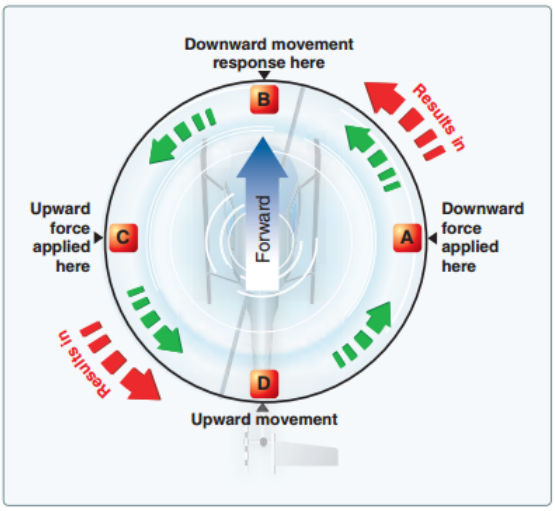

Figure 2.8: Gyroscopic precession [4]

Force Applied to Rotor Disk	Aircraft Reaction
Up at nose	Roll right
Up at tail	Roll left
Up on right side	Nose up
Up on left side	Nose down

Figure 2.9: Aircraft reactions to forces on a rotor disk [4]

2.3 Dissymmetry of lift

The rotation of rotor blades about the mast produces airflow with respect to the rotor blades. As the velocity of airflow across the rotor blade is highest at blade tips and reduces uniformly to zero at the center of the mast, the blade is designed normally with a twist to distribute the lifting force more evenly along the blade (figure 2.10).

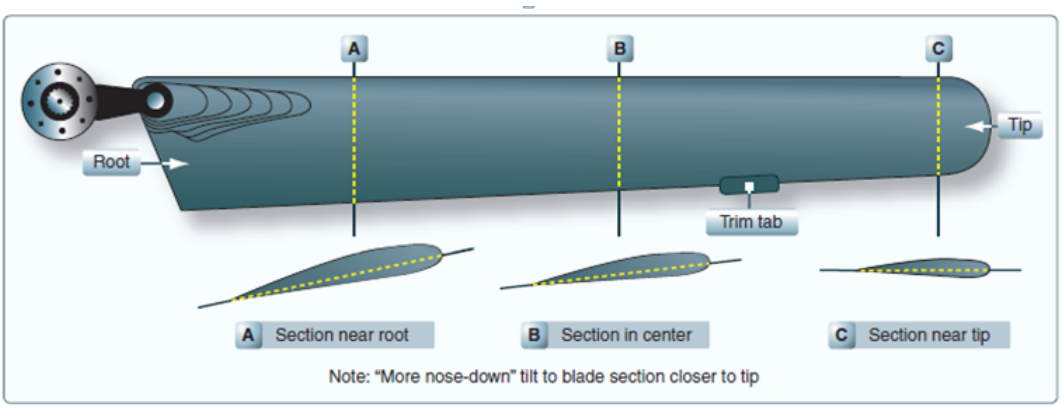

Figure 2.10: Blade twist [1]

In zero airspeed hover, the velocity of airflow across rotor blades depends on the rotor rotation velocity. However, in directional flight, the velocity of airflow across rotor blades becomes a combination of the rotational speed of the rotor and the airspeed of the helicopter. Figure 2.11 shows the velocity of airflow across the rotor blades in zero airspeed hover and forward flight. In forward flight, the relative airflow through the main rotor disc is greater on the advancing blade side than on the retreating blade side.

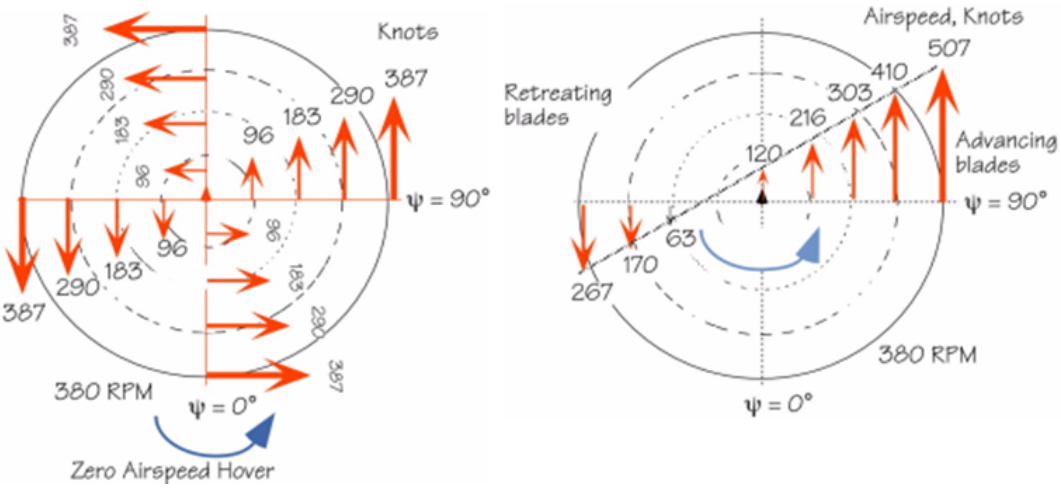

(a) Zero airspeed hover

(b) Forward flight

Figure 2.11: Velocity of airflow across rotor blades in zero airspeed hover and forward flight [2]

An example of forward flight is described in figure 2.12. The advancing blade, in position A, moves in the same direction as the helicopter. The velocity of relative airflow or relative wind respect to the blade is increased by the forward airspeed of the helicopter. The retreating blade, in position C, moves in the opposite direction of the helicopter. The velocity of the airflow meeting this blade is decreased by the forward airspeed of the helicopter. Therefore, the lift on the advancing blade side of the rotor disc is greater than the lift over the retreating blade side (figure 2.13). Due to the dissymmetry of lift, a helicopter with a counterclockwise main rotor rotation would roll left in forward flight, if a compensation was not introduced.

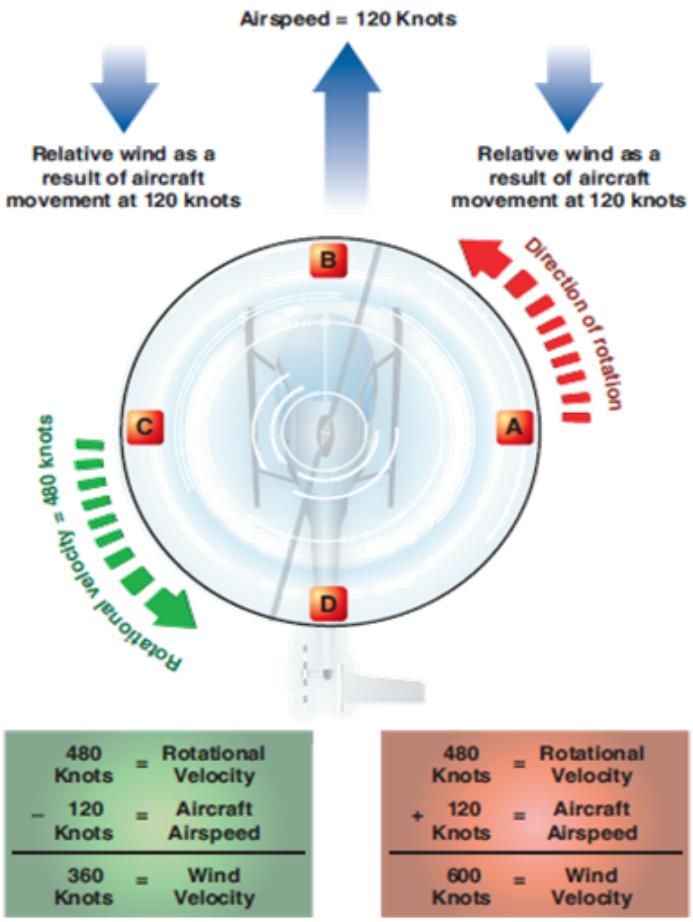

Figure 2.12: Airflow in forward flight [1]

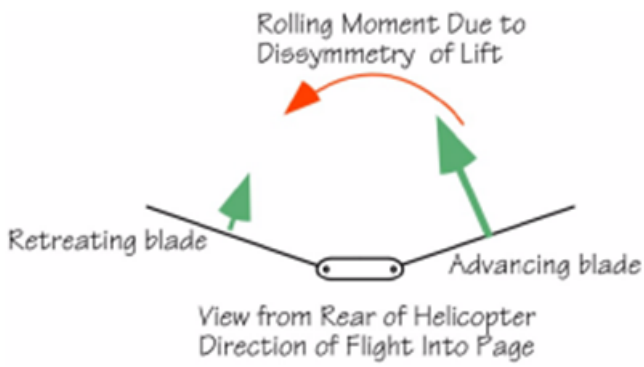

Figure 2.13: Dissymmetry of Lift [2]

2.3.1 Blade flapping

The dissymmetry of lift is compensated by blade flapping. The rotor system contains a flapping hinge which allows the rotor blades to flap up or down, as they rotate. Figure 2.14 describes the flapping phenomenon that compensates the dissymmetry of lift. Assuming that the blade pitch angle remains constant, in forward flight, lift increases on the advancing blade (position A), which causes the blade to

flap up. The up flapping velocity reduces the angle of attack of the blade which decreases the lift on the advancing blade. On the retreating blade (position C), the forward speed reduces lift and the blade flaps down. This phenomenon introduces a down flap velocity, which increases the angle of attack of the retreated blade. The retreating blade increases thus the lift thanks to the flapping phenomenon.

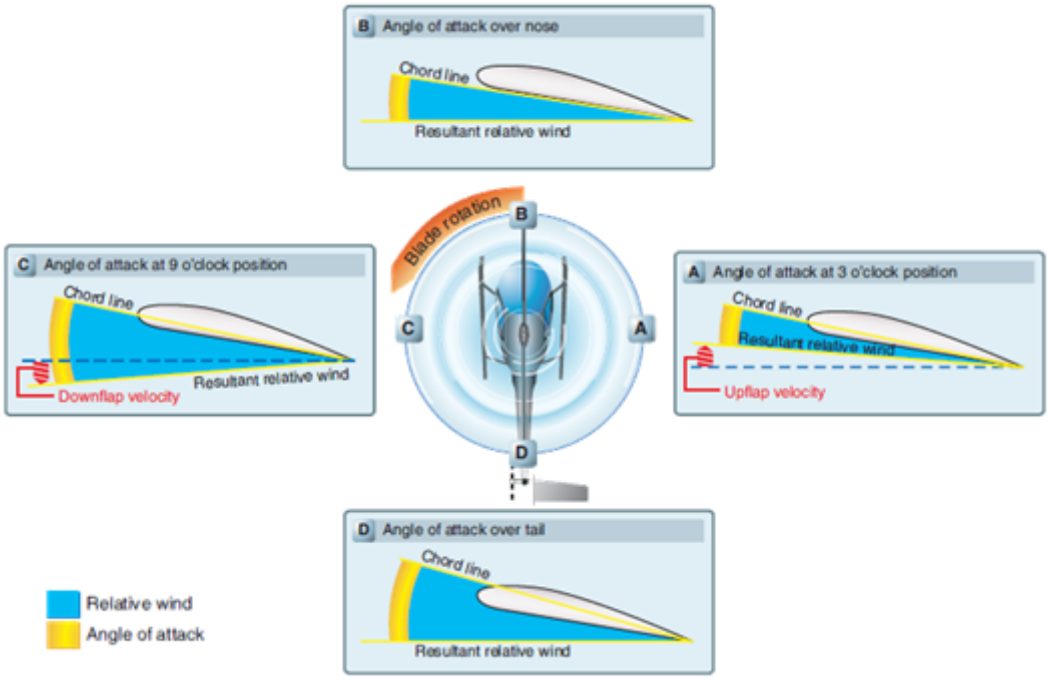

Figure 2.14: Flapping phenomenon [1]

2.3.2 Retreating blade stall and never-exceed speed (VNE)

In the forward flight, lift decreases on the retreating blade and the compensation is made by increasing the angle of attack due to flapping. However, the retreating blade stalls when the angle of attack exceeds the critical angle of attack. Therefore, pilots avoid retreating blade stall by not exceeding the never-exceed speed, V_{NE}.

2.4 Helicopter flight control

For a typical helicopter, there are four flight controls that the pilot uses during flight: collective pitch, cyclic pitch, throttle and anti-torque. Figure 2.15 presents the location of each control inputs in the helicopter. This section describes how each control inputs are used to flight a helicopter.

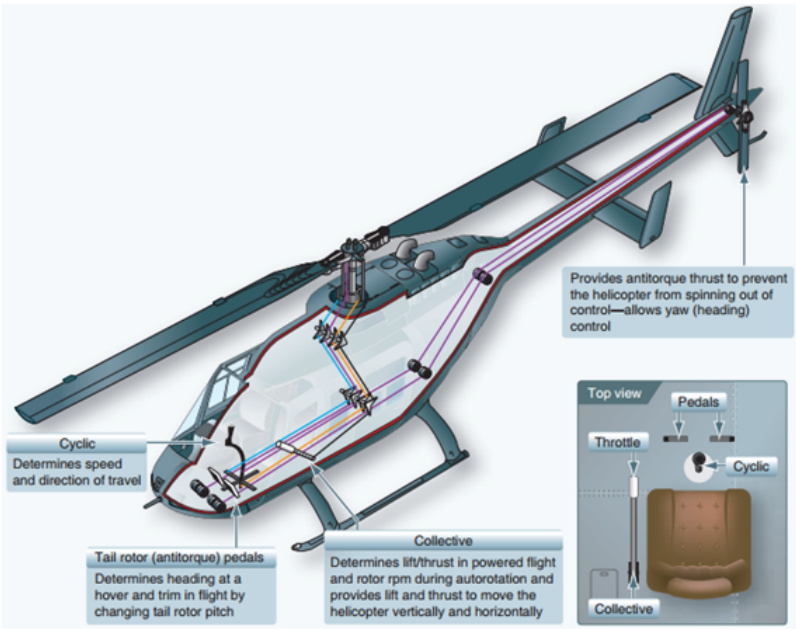

Figure 2.15: Major controls in the helicopter: collective pitch, throttle, cyclic pitch, and anti-torque [4]

2.4.1 Collective control

Collective pitch control, or collective lever, is located by the left side of the pilot's seat and is operated with the left hand. The collective is used to change the pitch angle of all the main rotor blades simultaneously, which allows the helicopter to increase and decrease its total lift-thrust intensity without changing its direction. Therefore, the collective control is mainly used to control the altitude of the helicopter. In a hovering flight, it maintains the altitude of the helicopter and, in a vertical flight it enables the helicopter to climb and descent.

When the collective control is performed, it changes the angle of incidence of the rotor blades and hence the angle of attack of the main rotor blades. Changing the angle of attack changes the drag on the rotor blades, which affects number of revolution per minute (RPM) of the main rotor. When the collective lever is raised to increase the pitch angle of all rotor blades, angle of attack increases, drag increases, rotor RPM and engine RPM tend to decrease. Lowering the collective lever decreases the pitch angle, hence, decreases angle of attack and drag while rotor RPM tend to increase. Since it is essential that the rotor RPM remain constant, a proportionate change in power is required to compensate the change in drag. This can be accomplished with the throttle control, which automatically adjusts engine power. This increases power when the collective pitch level is raised and decreases power when the level is lowered.

2.4.2 Throttle control

The throttle controls the power of the engine and it is used to maintain the rotor speed constant whenever the RPM of the main rotor is affected by collective inputs.

2.4.3 Cyclic control

The cyclic pitch control is usually located between the pilot's legs or between the two pilot seats. As already mentioned, the total lift-thrust force is always perpendicular to the tip-path plane of the main rotor. The cyclic pitch control can be used to tilt the rotor disc, which changes the pitch angle of the rotor blades cyclically and provides thrust in the direction the rotor is tilted. This phenomenon controls the direction of the total-thrust lift, which allows the helicopter to move in any directions: forward, rearward, left, and right (figure 2.16). The cyclic control is mainly used to control the attitude and airspeed of helicopter. Because the rotor disk acts like a gyro, the mechanical linkages for the cyclic control rods are rigged in such a way that they decrease the pitch angle of the rotor blade approximately 90 degrees before it reaches the direction of cyclic displacement, and increase the pitch angle of the rotor blade approximately 90 degrees after it passes the direction of displacement [1].

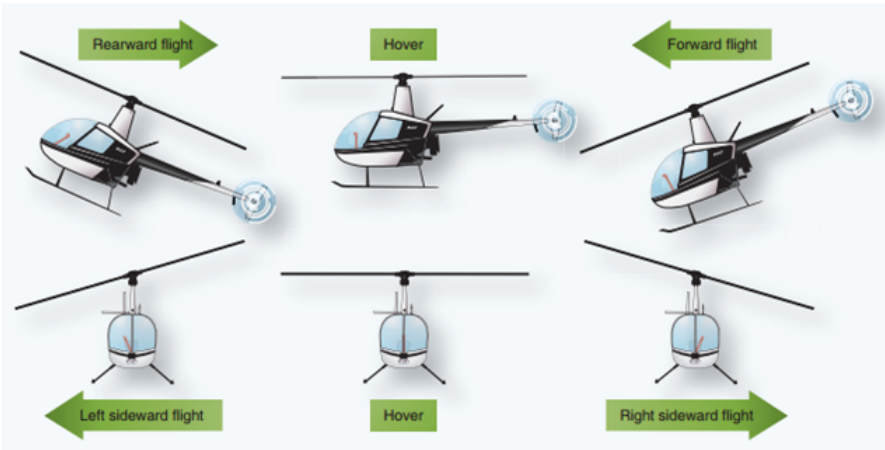

Figure 2.16: Cyclic control and the main rotor disc position [4]

2.4.4 Anti-torque pedals or tail rotor control

As the engine rotates the main rotor system in one direction, the helicopter fuselage tends to rotate in the opposite direction. This effect is called torque and the amount of torque is directly related to the amount of engine power being used to turn the main rotor system. Most helicopters use anti-torque or tail rotor to compensate the reaction torque. The tail rotor produces thrust in the direction opposite to torque reaction developed by the main rotor. The anti-torque pedal in the cockpit permits the pilot to change the pitch angle on the tail rotor blades in order to control the thrust. The tail rotor serves as well to control helicopter heading during flight. Application of more control than is necessary to counteract torque will cause the nose of helicopter to turn in the direction of pedal movement. From the neutral position, applying right pedal causes the nose of the helicopter to yaw right and the tail to swing to the left. Pressing on the left pedal, the nose of the helicopter yaws to the left and the tail swings right (figure 2.17) [1].

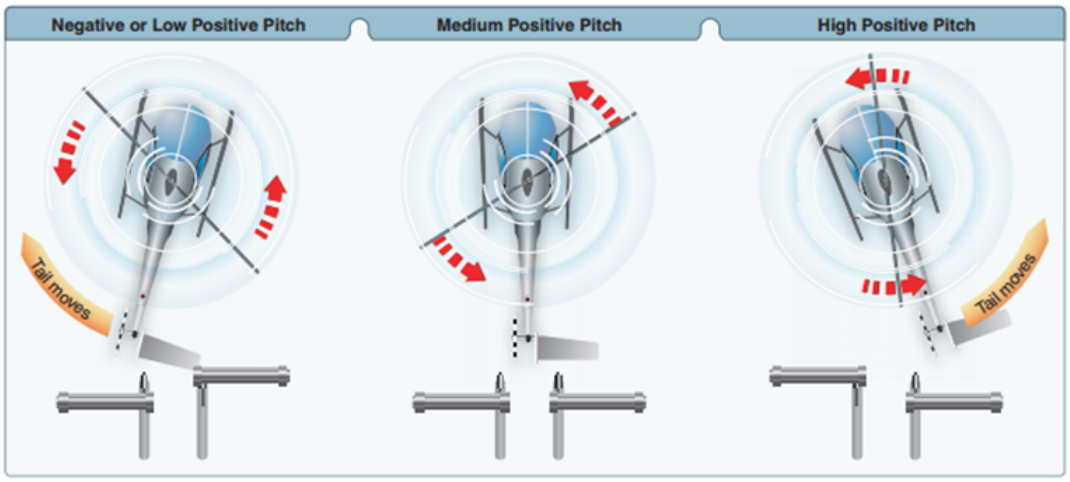

Figure 2.17: Tail rotor pitch angle and thrust in relation to pedal positions during cruising flight [1]

3 Automatic Flight Control System (AFCS)

An Automatic Flight Control System (AFCS) can be used to control and guide a helicopter without constant "hands-on" control by human being required. Hence, this system can take over some parts of the pilot's routine task, such as maintaining an altitude, climbing or descending to an assigned altitude, turning to and maintaining an assigned heading. Three types of systems in AFCS for helicopter are presented in this chapter.

3.1 Stability Augmentation System (SAS)

The automatic flight control system includes the Stability Augmentation Systems (SAS), such like pitch, roll and yaw SAS. Selecting SAS mode in APCP (Autopilot Control Panel) increases the stability on pitch, roll and yaw axes of the helicopter by increasing the damping ratio through the application of feedback control. Moreover, it enhances pilot control motions while helicopter motions caused by outside disturbances are counteracted. Therefore, this mode of operation improves the basic helicopter handling qualities.

3.2 Attitude Retention System (ATT)

While SAS is a "hands-on" flying mode, ATT is the basic "hands-off" Autopilot(AP) mode. The attitude retention systems such as Pitch, Roll, Yaw attitude control form the essential functions of any AFCS, they allow an aircraft to be placed, and maintained, in any required, specified orientation in space, either in direct response to pilot's command, or in response to command signals obtained from an aircraft guidance systems.

When the ATT mode is engaged, the existing attitude at the moment of its engagement is maintained. Changes in attitude can be accomplished usually by Cyclic Beep Trim (CBT) switch or Force Trim Release (FTR) switch, which set the desired attitude manually. The beep trim switch is used to adjust small attitude changes while the FTR switch moves the helicopter to fly the desired new attitude. Upon release of the selected switch, the autopilot will provide commands to hold the new attitude.

Stability augmentation systems, often form the inner loops of attitude control systems, an example of SAS and ATT for pitch axis is shown in figure 3.1, where θ_{ref} is the reference of the pitch angle, θ is the pitch angle, q is the pitch rate, K_θ and K_q are the gains.

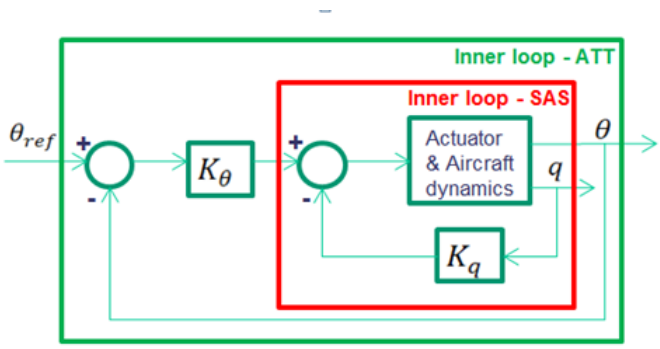

Figure 3.1: Representation of the SAS and ATT for pitch axis

3.3 Autopilot and Flight Director (AP/FD)

To decrease the pilots charge, autopilot systems provide for "hands off" flight along specified lateral and vertical paths [10]. The functional modes that are called "Flight Director (FD)" modes may include IAS (Indicated Airspeed), HDG (Heading), ALT (Altitude), VS (Vertical speed) , NAV (Navigation), APPR (Approach), etc. These modes can operate independently, controlling airspeed, heading and altitude, or it can be coupled to a navigation system and fly a programmed course or an approach.

The FD modes are generally used in direct connection with the Autopilot (AP). As shown in figure 3.2, the FD commands the AP to put the aircraft in the attitude necessary to control flight parameters like altitude, airspeed, heading, vertical speed, etc., in order to fly a given trajectory. For example, selecting the IAS mode, the AFCS acts as a feedback regulator to track and maintain the helicopter speed at a reference value by sending command signals to the attitude control system.

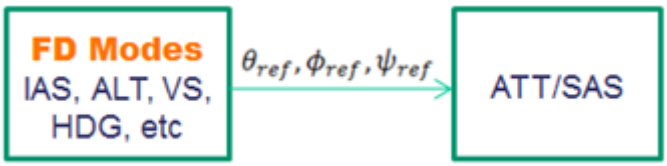

Figure 3.2: Connection between ATT/SAS and FD modes

4 The internship context

An AFCS contains several autopilot modes which are used to control the movement of the helicopter in longitudinal, lateral and vertical direction. For instance, if the IAS mode is engaged, the longitudinal control is performed to control the airspeed of a helicopter. With ALT mode engaged, the vertical flight parameter, altitude, can be controlled.

The AFCS considered in this study has a base tuning biased towards performance. However, when an aircraft encounters atmospheric turbulence, turbulence affects the accelerations of the helicopter in different directions, and the AFCS is not optimised for such conditions. Passengers may experience discomfort due to the changes in acceleration encountered during flight. Moreover, ineffectual corrective command may be generated by AFCS.

When the AFCS is used to maintain a selected airspeed (IAS mode engaged), a comparison between the selected airspeed and the measured airspeed is performed, and the difference between these two quantities is defined as the velocity error. In case the velocity error is not zero, the control system creates a corrective command, to increase or decrease the airspeed of the aircraft, in order to achieve a zero velocity error. The change of air flow caused by turbulence alters the airspeed, which creates a velocity error that the AFCS attempts to eliminate. In the meanwhile, the effect of turbulence alters the inertial velocity (longitudinal ground speed) as well, due to the drag force of the air flow. Nonetheless, the command action applied by AFCS does not erase the inertial accelerations coming from turbulence conditions, but instead deteriorates them. An example from a US patent [5] is commented below to illustrate the fact mentioned.

A typical closed-loop of airspeed control system presented in the prior art of invention [5] is shown in figure 4.1. The system defines the airspeed error as the difference between the airspeed command and the measured airspeed. The airspeed error signal is sent to actuators and the control system operates actuators to reduce this airspeed error to zero. For a fixed-wing aircraft, the control system will command a change in the throttle position. Figure 4.2 contains graphics over time of the input and response for a transient head-on gust. Figure 4.2 a) presents a 30ft/sec head-on gust that is encountered for 5 seconds. As shown in figure 4.2 b), the airspeed sensor detects an increase in airspeed due to the gust at the instant of 5 seconds. While the airspeed augments, the ground speed, in figure 4.2 c), decreases. In response to the increased airspeed, the velocity control system commands a change in throttle position, figure 4.2 d), to reduce engine power in order to bring the airspeed to the original one, around 200 knots. As a result, the airspeed starts to drop at about 7 seconds and the aircraft is decelerated to an even slower ground speed. When the gust ceases at 10 seconds, the airspeed falls below 200 knots due to the reduction of head-on gust. In the meantime, the ground speed starts to rise. The control system detects airspeed error and changes the throttle position to accelerate the aircraft in order to reach the original airspeed. However, the aircraft is accelerated to an even higher ground speed. Thereby, the deceleration and acceleration caused by a transient gust are worsened by the throttle command action, as exposed in figure 4.2 e).

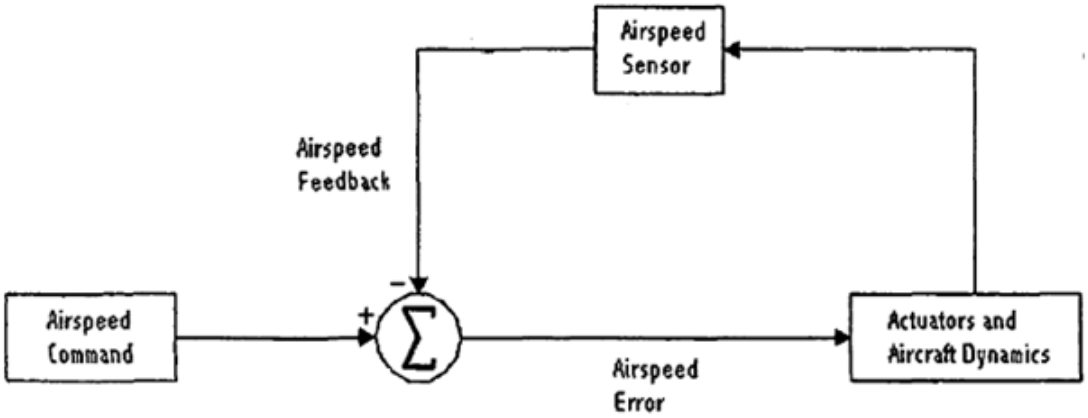

Figure 4.1: Typical airspeed control system presented in the prior art of invention [5]

In a turbulent air environment, a typical speed control system creates additional accelerations apart from those caused by turbulence. In order to increase passengers comfort in turbulent air, the speed control activity should be reduced in order to minimize the longitudinal acceleration encountered in turbulent air. However, tuning the speed control system is a compromise between performance and comfort. On the one hand, it is desired to maintain the airspeed around the selected one, in order to achieve desired performance in calm air. Hence, the control system must be reactive to correct any velocity deviation, but it makes the flight less comfortable in turbulent conditions. On the other hand, the passenger comfort can be increased in turbulent air if the control activity is reduced, but this approach will lead to a loss in performance in calm air.

4.1 Proposed methodology

If turbulence detection can be achieved, one can always select the best tuning for turbulent and calm environments, and therefore, it is no longer necessary to make a compromise between performance and comfort.

The base tuning considered is biased towards performance. Therefore, the objective of the internship is to seek another tuning of the speed control system, which should be dedicated mostly for comfort issue, in a turbulent condition. Then, the turbulence detection mechanism should be developed to select the more reactive controller when flying in calm air, and switch to the more damped controller when flying in turbulent air.

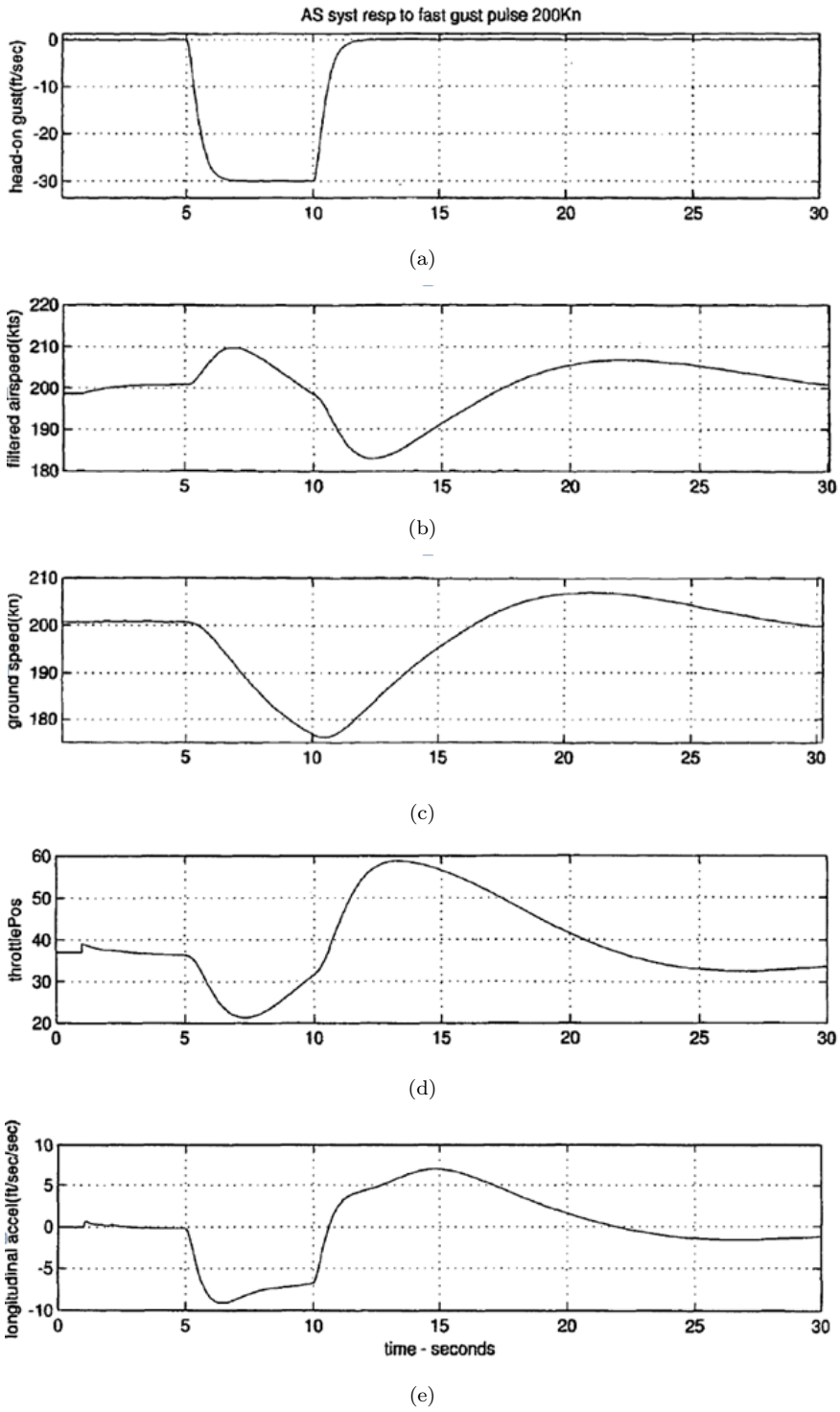

Figure 4.2: The input and response of a transient head-on gust from the invention [5] by using the control system of figure 4.1

5 Bibliographic research

The focus of this internship is to modify the control system to reduce turbulence effects on the helicopter. Before attempting to implement potential solution, it is important to investigate the state of the art on this topic and investigate the existing control law adopted for turbulence conditions, in order to help us to seek for alternative solutions. The first subsection presents the papers relative to the control law for minimizing turbulence disturbances. In addition to the first part of bibliographic research, it is useful to have a comfort evaluation criterion to evaluate the improvement achieved by the modified control system when compared to the original one. Therefore, the second part of the bibliographic research is dedicated to the comfort evaluation method based on ISO (International Organization for Standardization) standard 2631-1.

5.1 Existing control law for minimizing turbulence disturbances

The bibliographic research about the reduction of turbulence effects on aircraft reveals a small number of materials. Two documents relative to this subject were found. The first paper [6], from a US patent, presents a throttle control system that compensates velocity disturbances caused by turbulence. The second paper [5], also from a US patent, introduces a velocity control system that reduces undesirable accelerations encountered in turbulent atmosphere. Both papers are directed to the aircraft throttle control system, but the same principle can be applied to a helicopter speed control system.

5.1.1 US patent 4422147 - Wind shear responsive turbulence compensated aircraft throttle control system

The objective of the invention [6] is to provide an aircraft automatic throttle control system that maintains the aircraft at or near desired airspeed when the aircraft is subjected to atmospheric disturbances, including turbulence and wind shear.

It is known that the aircraft experiences abrupt changes in airspeed when it encounters turbulent conditions. The invention aims to structure the throttle control system to provide a very rapid and precise response, in order to correct quickly airspeed disturbances due to turbulence. In addition, the invention intends to obtain adequate system damping to ensure that a change in propulsive thrust results in smoothly varying the throttle control. Therefore, a multichannel throttle control system is proposed in [6], which utilizes both airspeed and the inertial acceleration signal as control parameters. The control system of the invention is shown in figure 5.1, which includes a speed command channel (14), a turbulence compensation channel (16) and a wind shear correction unit (12). However, the study was focused mainly on the speed command channel and the turbulence compensation channel.

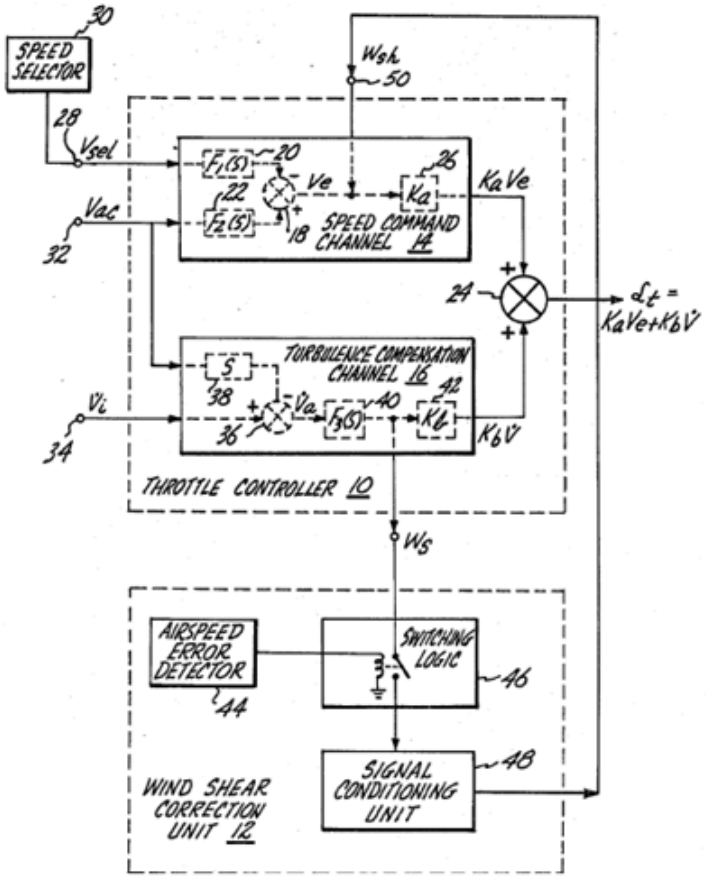

Figure 5.1: Automatic throttle control system of the invention [6]

According to [6], the automatic throttle control system in figure 5.1 is characterized by the following control law.

$$\delta_t = K_a V_e + K_b \dot{V} \tag{5.1}$$

δ_t in equation 5.1 represents the throttle command signal, K_a and K_b are gain factors. The airspeed error V_e is a difference between the actual airspeed (V_{ac}) and the selected airspeed (V_{sel}), while $\dot{V}$ is a difference between the longitudinal inertial acceleration ($\dot{V}_i$) and the derivative of the airspeed (sV_{ac}). The signal $\dot{V}$ from the turbulence compensation channel (16) is representative of airspeed disturbances due to atmospheric conditions. When the airspeed decreases (increases) due to a change in thrust, the longitudinal inertial acceleration decreases (increases) as well. Therefore, the signal sV_{ac} and $\dot{V}_i$ have the same algebraic sign and tend to cancel each other. However, in the presence of atmospheric disturbances, a decrease (increase) in airspeed is accompanied by a positive (negative) inertial acceleration. The signals sV_{ac} and $\dot{V}_i$ have the opposite algebraic sign and tend to sum up. Therefore, this control system stated in [6] can provide a rapid corrective change in airspeed, in order to respond to abrupt change in airspeed caused by turbulence. Moreover, with the throttle command signal decreasing as a result of the diminished airspeed error and the corrective acceleration term, ineffectual throttle activity can be reduced.

5.1.2 US Patent 7931238 B2 - Automatic velocity control system for aircraft

The second paper from [5] is related to an automatic flight control system for controlling the velocity of an aircraft. As presented earlier, a typical closed-loop system for controlling airspeed, in the prior art of invention [5], operates fairly well in calm air but in the presence of turbulent air, it creates additional accelerations apart from those caused by turbulence. The invention [5] is directed to an airspeed control system that minimizes the undesirable accelerations due to air turbulence encountered during flight.

The airspeed control system of this invention uses the combination of the airspeed signal and the inertial velocity (longitudinal ground speed) signal as the velocity feedback signal, figure 5.2.

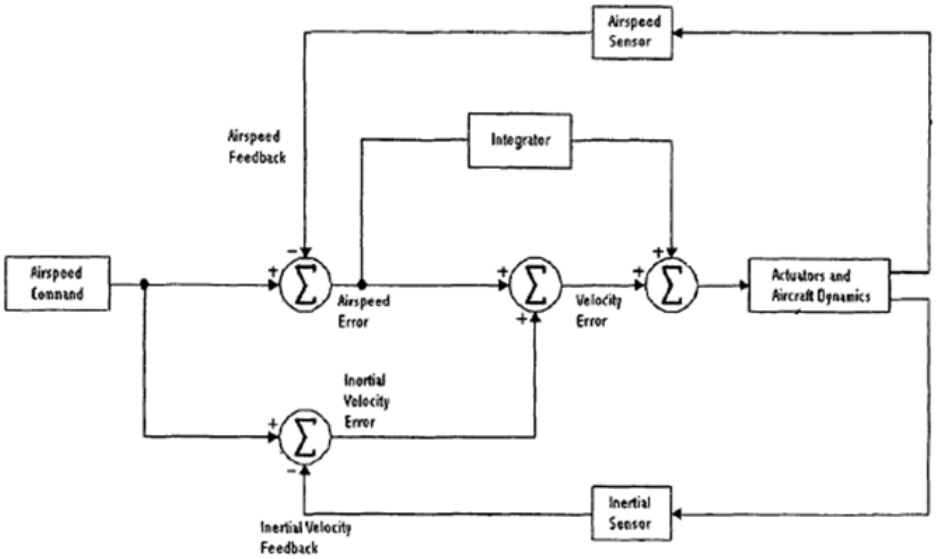

Figure 5.2: Airspeed control system of the invention [5]

The velocity error V_{error} in the airspeed control system according to figure 5.2 from [5] is defined by equation 5.2, where V_{ref} is the airspeed reference, V_a is the measured airspeed and V_i is the measured inertial velocity. Considering the first term $(V_{ref} - V_a)$ is the primary error and the second term $(V_{ref} - V_i)$ is the secondary error, the actuator command signal is defined as the sum of velocity error and an integrated value of the primary error signal.

$$V_{error} = (V_{ref} - V_a) + (V_{ref} - V_i) \tag{5.2}$$

It is known that airspeed is the forward velocity of the aircraft relative to the air mass in which the aircraft is flying, whereas inertial velocity is the forward velocity of the aircraft relative to the ground over which the aircraft is flying. When a wind gust is encountered, airspeed and inertial velocity changes in opposite direction, as already illustrated earlier. Thus, the velocity error obtained from the combination of airspeed and inertial velocity reduces the amplitude of the throttle command due to the cancellation of these two signals. As a result, the undesirable power or thrust is significantly less as well as the undesirable acceleration. The integral of the primary velocity error $(V_{ref} - V_a)$ is summed to velocity error to generate the actuator command signal, so the airspeed at steady-state is not affected by the inertial signal.

Compared to the responses (figure 4.2) given by the speed control system of figure 4.1, the curves from figure 5.3 show the improved response for a transient head-on gust using the control system of figure 5.2. The reduction of undesirable throttle command and longitudinal acceleration is verified in the figures 5.3 d) and e). Furthermore, this system, unlike the control system of figure 4.1, settles velocity deviations sooner without long oscillations, as portrayed in figure 5.3 b).

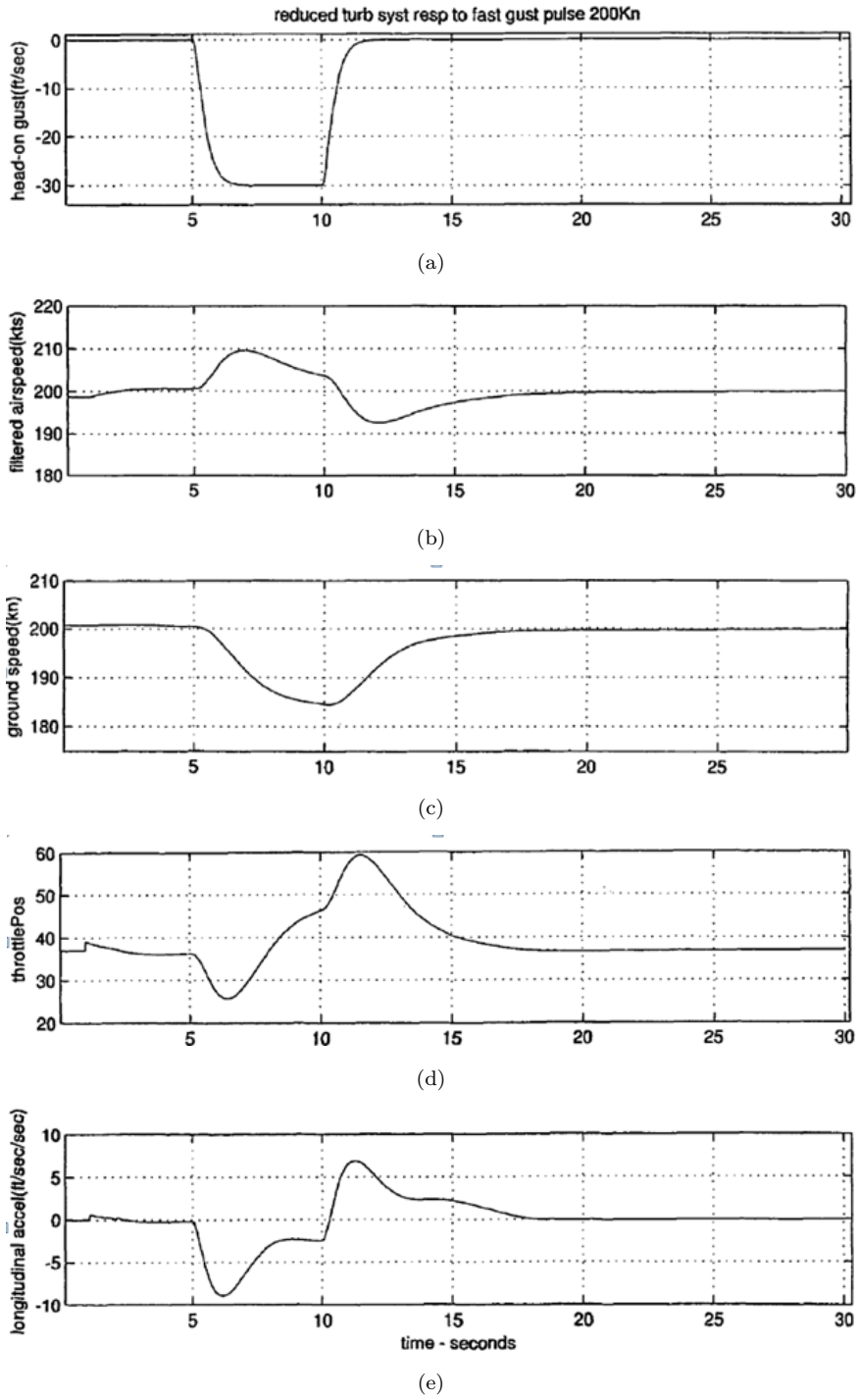

Figure 5.3: The input and response of a transient head-on gust from the invention [5] by using the control system of figure 5.2

5.2 Vibration exposure measurement and comfort evaluation

The existing standards VDI (Association of German Engineers) and ISO (International Organization for Standardization) define methods for evaluating and measuring the whole-body vibration on human concerning different aspects: Health risk, Comfort, Perception and Motion Sickness. Effects of whole-body vibrations on health, activities, perception and comfort are often associated with frequency from 1 to 100 Hz. Oscillations in this range of frequency are called vibrations in existing standards (e.g., ISO 2631-1, 1997; VDI 2057-1, 1987). Movements with frequencies below 1 Hz are denoted as motions and the principal effect of these oscillations is a kind of motion sickness. Whether a motion or vibration causes annoyance, discomfort or interferes with activities depends on many factors - including the characteristics of the presented vibrations like frequency components and levels, characteristics of the exposed person and many other aspects of the environment. Therefore it is difficult or impossible to summarize all effects, to define a standard with limits and standard values for all conditions and for the whole frequency and level range [8].

This section of the bibliographic research describes comfort criteria based on ISO 2631-1 standard, where "low frequency" comfort (vibrating comfort) and "very low frequency"' comfort (motion sickness phenomenon) criteria for aeronautics field are presented [11].

According to ISO 2631-1, "low frequency" comfort evaluation is based on the measurement of the acceleration felt by a passenger at the location where the body is in contact with the vibrational surface. During whole-body vibration in aircraft flight environments, the vibration of the aircraft is usually transmitted to the human body via the seating system and the main contact surfaces for a seated person include seat pan, seat back and feet. For a seated person, the orientation of the axes for measuring the vibration at each contact surface is presented in figure 5.4.

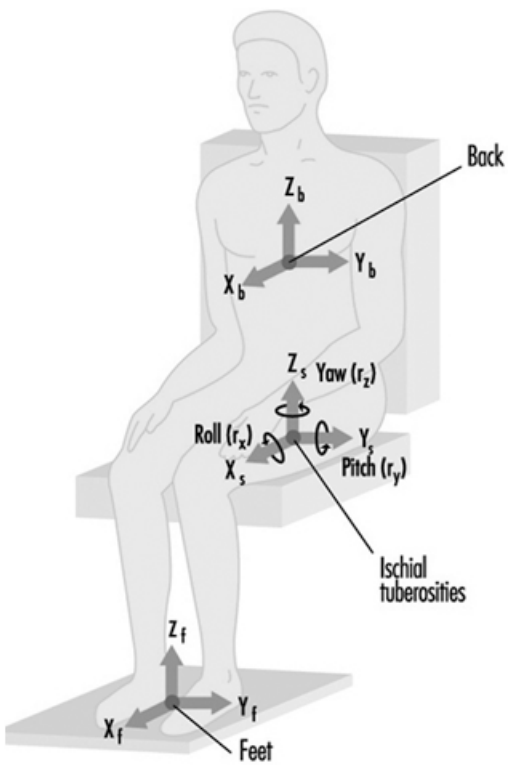

Figure 5.4: Axes for measuring vibration exposures for a seated person [7]

In order to represent the physiologic sensitivity of human body to vibration, a frequency weighting filter is introduced. The measured acceleration is filtered with frequency weighting curves specified by the standard, to correlate the vibration measurements to a person response to vibration. For a seated person, two frequency weighting curves are used, for vertical (z axis) and lateral (x and y axis) acceleration, as the human body has the same sensitivity for vibrations in x and y directions according to ISO 2631-1.

The curves W_k and W_d in figure 5.5 correspond respectively to the acceleration weighting curve for vertical seat vibration (z axis) and the acceleration weighting curve for horizontal seat vibration (x and y axis). As one can observe, the curves W_k and W_d emphasize the frequency range between 4 to 8 Hz for vertical acceleration and 1 Hz for the lateral ones. The curve W_f in figure 5.5 correspond to the acceleration weighting curve that is used to evaluate motion sickness on vertical axis. The comfort evaluation concerning motion sickness will be presented later.

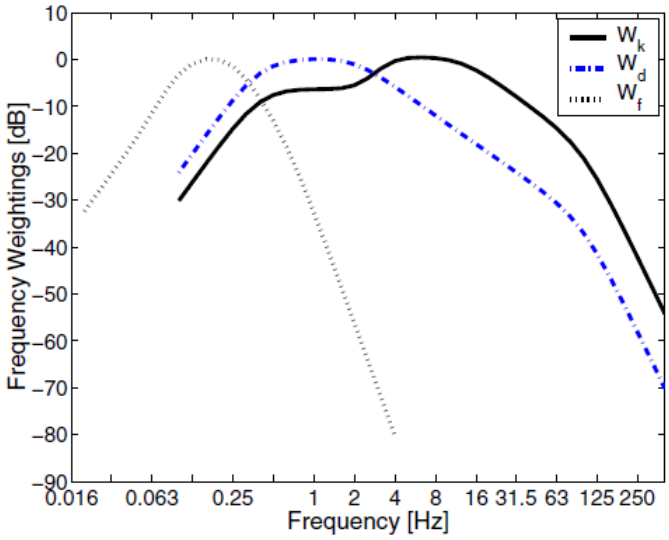

Figure 5.5: Frequency weighting curves defined in ISO 2631-1 (1997) [8]

The standard evaluates a random vibration signal by using the Root Mean Square (RMS) value [11]. The RMS of the frequency weighted acceleration for each component of the acceleration is computed by using equation 5.3, where a_w (m/s^2) is the instantaneous frequency weighted acceleration and T, the length of time over which the RMS value is being computed.

$$\bar{a_w} = \left[\frac{1}{T}\int_0^T a_w^2(t)dt\right]^{\frac{1}{2}} \tag{5.3}$$

The total vibration value a_v at a measurement point can be computed from the RMS values of weighted accelerations in each axis, as shown in equation 5.4.

$$a_v = ({k_x}^2{a_{wx}}^2 + {k_y}^2{a_{wy}}^2 + {k_z}^2{a_{wz}}^2)^{\frac{1}{2}} \tag{5.4}$$

Where:
a_{wx}, a_{wy}, a_{wz} are RMS values of the weighted acceleration on x, y and z axes;
k_x, k_y, k_z are weighting factors; for a seated person the standard proposes the following factors:
-at the supporting seat surface: $k_x = 1$, $k_y = 1$, $k_z = 1$;
-at the feet: $k_x = 0.25$, $k_y = 0.25$, $k_z = 0.4$.

When comfort is affected by vibrations at several points, the overall vibration can be computed from RMS value of global vibrations at each point, as in equation 5.5.

$$a = ({a_{p1}}^2 + {a_{p2}}^2 + {a_{p3}}^2)^{\frac{1}{2}} \tag{5.5}$$

For a seated person, this involves the vibration measured at the supporting seat surface, at the feet and at the seat back. In addition, the comfort for a seated person may also be affected by rotational vibrations on the seat. However, for civil aircraft applications, rotational vibrations as well as the ones transmitted by the back of the seat may be neglected [11].

In reference to comfort, the acceptable values of vibration magnitude depend on many factors which vary with trip duration and type of activities passengers expect to accomplish. The standard gives approximate indications of the likely reactions to various magnitudes of overall vibration value (a in m/s^2) in public transport (see figure 5.6).

weighted acceleration a [m/s^2]	(Dis-) comfort categories
< 0.315	not uncomfortable
0.315 to 0.63	a little uncomfortable
0.5 to 1	fairly uncomfortable
0.8 to 1.6	uncomfortable
1.25 to 2.5	very uncomfortable
> 2	extremely uncomfortable

Figure 5.6: Scale of vibration (dis-) comfort adapted from ISO 2631-1 (1997) from [8]

Concerning the motion sickness phenomenon, “very low frequency” comfort, the standard is based on vertical acceleration felt by a human passenger. As for “low frequency” comfort, there is also a frequency weighting function for representing human sensitivity to motion sickness. The curve W_f in figure 5.5 corresponds to the acceleration frequency-weighting curve for vertical motion sickness.

The ISO 2631-1 standard proposes to compute a motion sickness index representative of the Percentage of Ill Passengers (PIP). At first, the measured acceleration should be weighted by the frequency-weighting curve W_f in order to obtain the weighted acceleration, a_w (m/s^2). Then, a cumulative measure of acceleration or ”acceleration dose value” can be calculated by using the equation 5.6, where T is the duration of the journey in seconds. Finally, the relation between acceleration dose value and PIP can be represented by equation 5.7. According to reference [12], this relation was obtained by linear approximation of experimental data. It is important to acknowledge the nature of the data from which the procedure has been developed since this defines the scope of application. See [11] for more information about the application of PIP to evaluate passenger comfort in a civil aircraft.

$$dose = \left(\int_0^T a_w^2(t)dt \right)^{\frac{1}{2}} \tag{5.6}$$

$$PIP = 1/3 * dose \tag{5.7}$$

In [11], the comfort criterion is applied to a large capacity civil aircraft for passenger comfort evaluation, in order to choose the best methodology for control law design. In this study, the criterion is applied to a helicopter, in order to quantify the improvements of the new control system.

6 Implementation and results

As previously mentioned, the purpose of this work is to increase passenger comfort, by reducing the accelerations encountered in a turbulent environment. Therefore, the followed methodology aims to reduce the AFCS control activity when the helicopter is operating in turbulent air.

As presented earlier, the speed control system, when operating in turbulent air, creates additional accelerations in the longitudinal direction; thereby the first part of this section presents the modifications introduced on the speed control system to minimize the longitudinal acceleration.

As already mentioned, using another tuning dedicated mostly for comfort issue in a turbulent condition requires a turbulence detection mechanism. This mechanism should be able to select the original speed controller in calm air, and to switch the controller to the one that increases comfort, in case of turbulence detection. The implementation of the turbulence detection mechanism in the AFCS is described in the section 6.2.

The section 6.3 deals with performance evaluation of the modified speed controller, in both calm air and turbulent air.

Finally, in the end of the chapter, the comfort evaluation method described in the section of bibliographic research is implemented to evaluate the improvement achieved by the modified control system.

6.1 Speed control activity reduction

A helicopter model provided by Thales is used for the implementations described above. The principal components of this model are: the helicopter dynamics model, the sensors models, the actuators models and the control laws.

A turbulence model used is included in the helicopter model, see [9] for more information about this model. Figure 6.1 and figure 6.2 present the turbulence scale lengths and intensities as a function of altitude.

Understanding how the speed control system operates and what its components are helps us to narrow a direction to where one should be looking for a solution. A simplified scheme of speed control loop is shown in figure 6.3. The Calibrated Airspeed (CAS) from Air Data Unit (ADU) model and the acceleration given by Attitude and heading reference system (AHRS) are filtered and combined to synthesize a velocity and an acceleration, denominated respectively VXBI and AXBI. This filtered velocity and acceleration are considered as feedback variables afterwards in the speed control law. The IAS control law generates the correction of pitch attitude according to the difference between the VXBI and the velocity reference. Finally, the attitude correction is sent to the ATT/SAS for generating cyclic inputs, in order to change the pitch attitude of the helicopter.

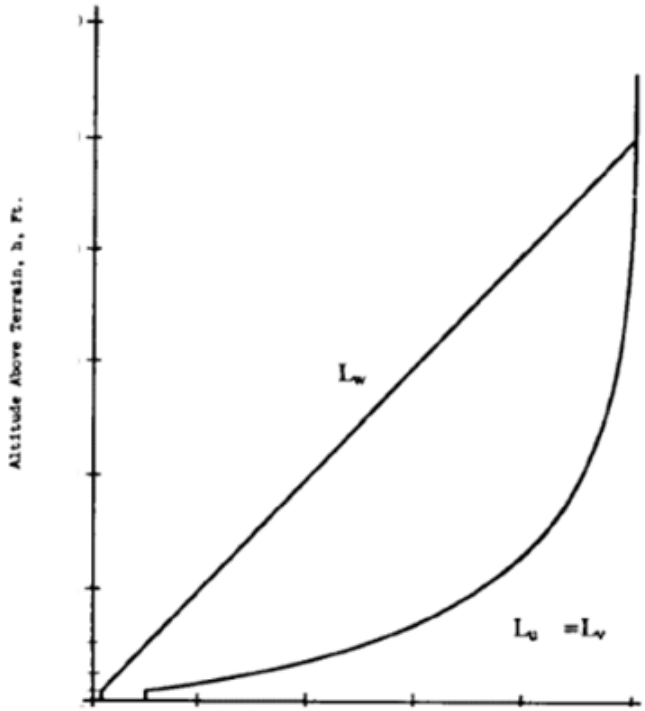

Figure 6.1: Turbulent Scale Lengths as function of altitude (10<h<1000ft) [9]

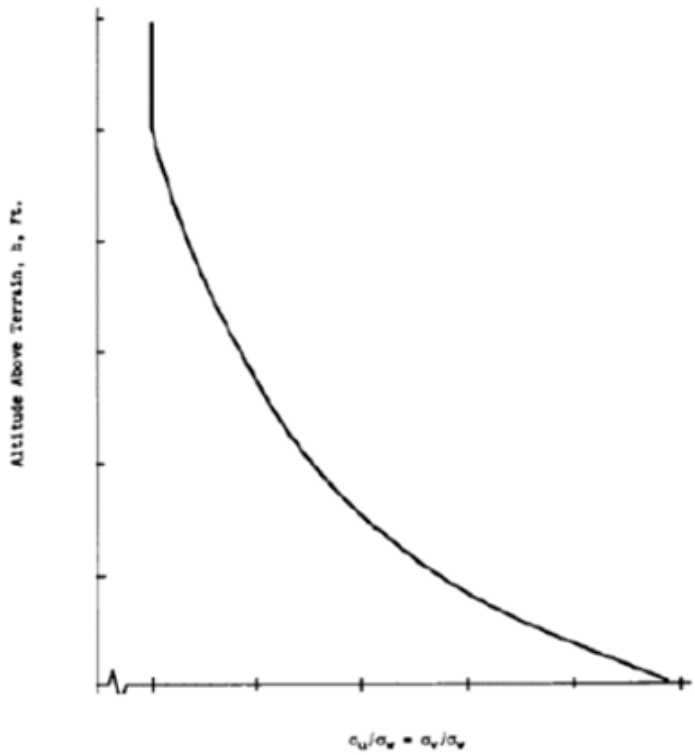

Figure 6.2: Turbulent Intensities as function of altitude (10<h<1000ft) [9]

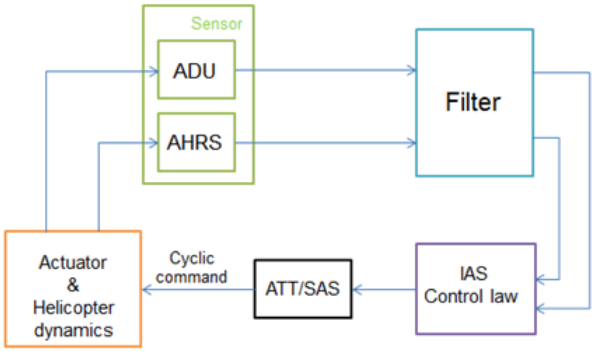

Figure 6.3: Simplified scheme of speed control loop

The helicopter operates fairly well in calm air with mode IAS, ALT and HDG engaged, as shown in figure 6.4.

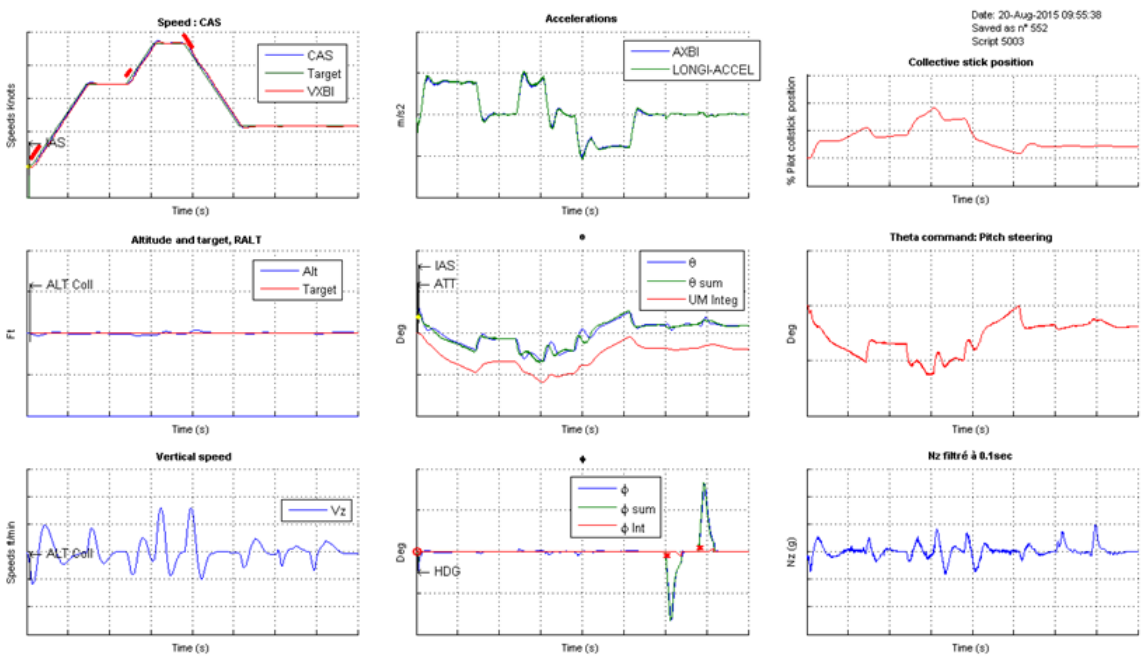

Figure 6.4: Response of the helicopter in calm air

It is known that in turbulent air, the turbulence changes the airspeed and the inertial velocity in opposite direction. With IAS mode engaged, the speed control system, in order to correct airspeed deviations, creates additional inertial accelerations apart from those caused by turbulence. Thus, the helicopter will experience acceleration changes. Moreover, ineffectual corrective commands may be generated in an attempt to correct the constant airspeed deviations caused by turbulence. Constant changes in control inputs and acceleration in a turbulence condition can be verified in the curves of figure 6.5: Pitch Steering, Collective stick position and Acceleration.

In order to minimize the accelerations on the helicopter, the first solution is to reduce control law gains. Smaller gains in control law make the speed control system less reactive to substantial velocity errors, and therefore the objective can be achieved. As shown in figure 6.6, the changes in longitudinal accelerations

and pitch command are reduced. However, as the control activity is reduced, the speed control system will provide slower response to eliminate velocity errors of any origin. Therefore, this approach causes a loss in performance, especially when a maneuver is performed. For example, when the airspeed changes are required, the speed control system does not react quickly to bring the helicopter to the velocity target. It can be seen in figure 6.7, the delay of the CAS with respect to the target is increased, when smaller gains are used in IAS control law.

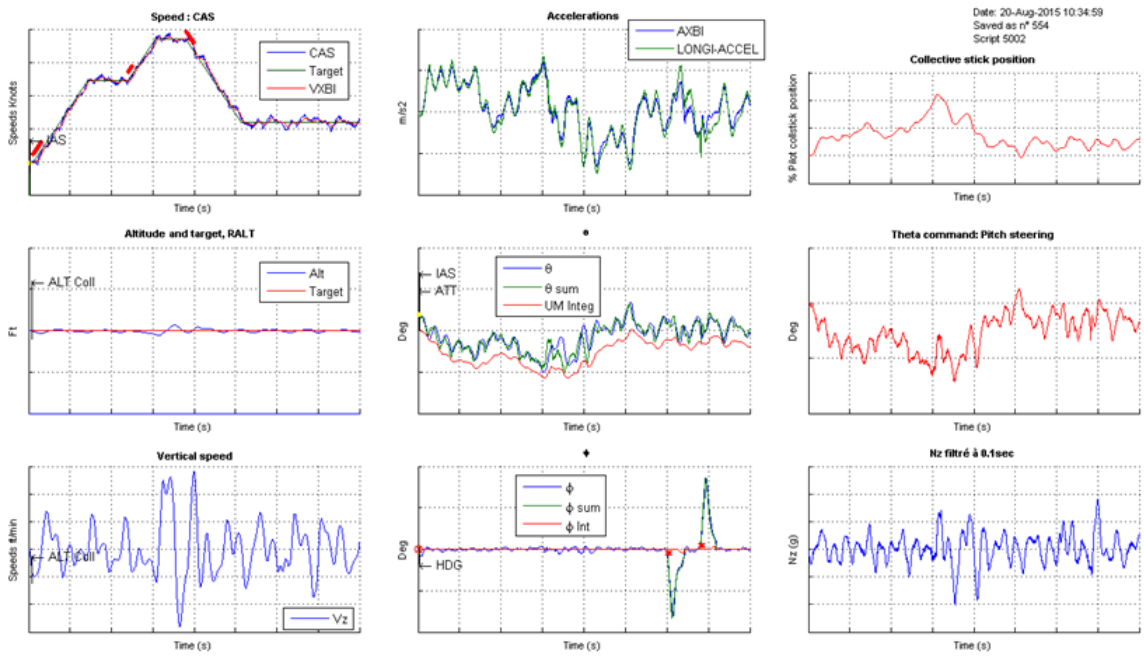

Figure 6.5: Response of the helicopter in turbulent air with the original speed control system

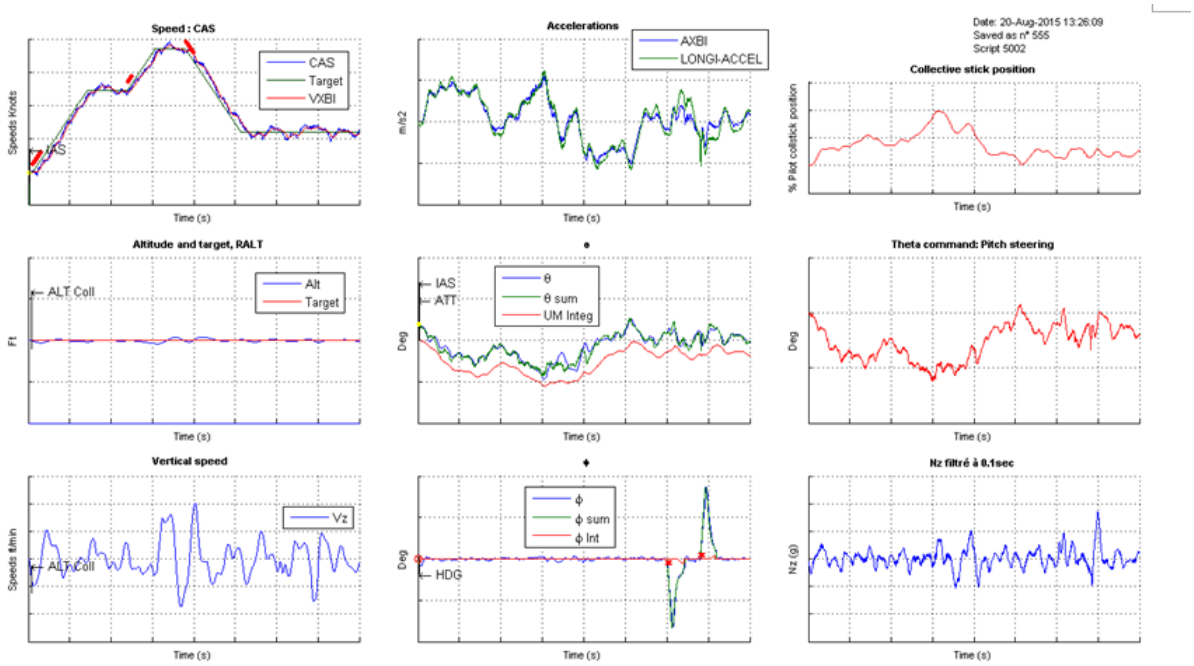

Figure 6.6: Response of the helicopter in turbulent air with reduced gains in the control law

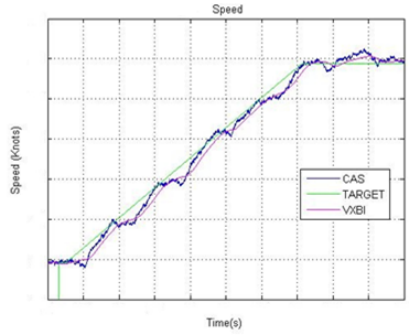

(a) Original gains in the control law

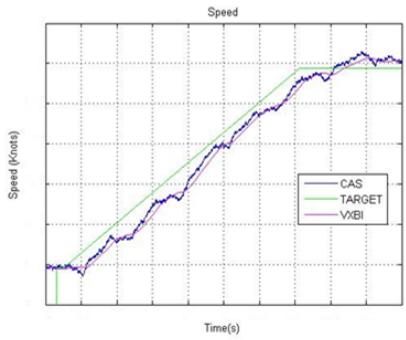

(b) Reduced gains in the control law

Figure 6.7: Speed response in turbulent air

The alternative solution focus on modifying the filter block placed before the IAS control law. It is known that the IAS control law generates the corrective command according to the velocity error, which is defined as the difference between VXBI and velocity reference. If the cut-off frequency of the filter is lowered, the velocity VXBI will track CAS slower and smoother, when "high frequency" of CAS deviation occurs. Therefore, the velocity error that is taken into account in the IAS control law will be less and the control activity of the speed control system will be reduced. Figure 6.8 presents three graphics of velocity in function of time, where the cut-off frequency of the velocity filter is reduced at each graphic. As one can observe, the response of the VXBI is smoother and the velocity errors is lower, as the cut-off frequency is reduced.

In case of the cut-off frequency is significantly reduced, the VXBI has difficulties to track CAS in frequencies higher than the cut-off frequency, which can compromise the performance of autopilot in some of these frequencies. The cut-off frequency in the velocity filter is adjusted to have reasonable improvement in comfort without compromising considerably the performance. Figure 6.9 confirms the improvement achieved by the modified filter with respect to the original filter presented in figure 6.5. Both changes in control inputs and inertial acceleration are reduced. Besides, the vertical response of the helicopter is also improved, as indicated in Vertical speed graphic and Nz graphic of figure 6.9. It is known that cyclic corrective inputs change constantly the amount of lift, which affects the vertical movement of the helicopter. In the simulated case, where ALT mode is engaged along with IAS, the collective input commands the helicopter to correct altitude disturbances introduced by turbulence and cyclic inputs. Reduction of speed control activity moderates cyclic control, which affects less the vertical movement of the helicopter. Therefore, the collective control activity is also reduced, which eliminates additional vertical accelerations.

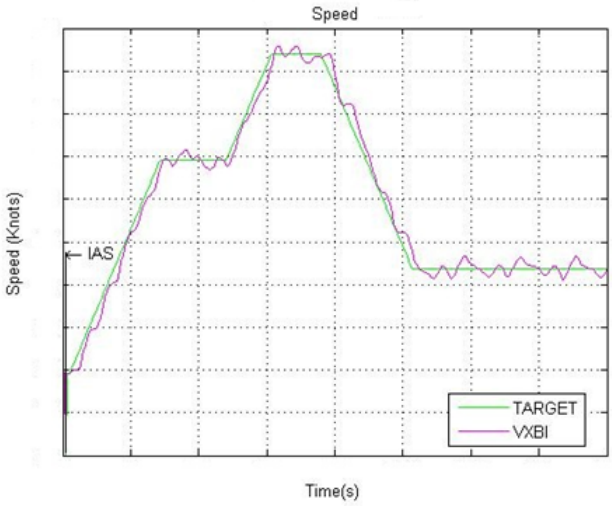

(a)

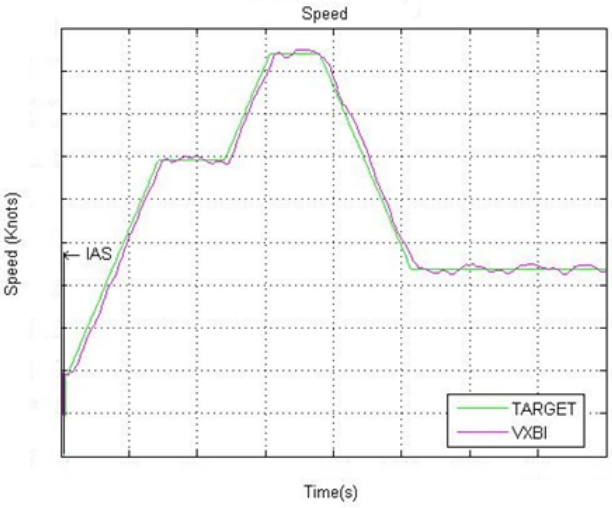

(b)

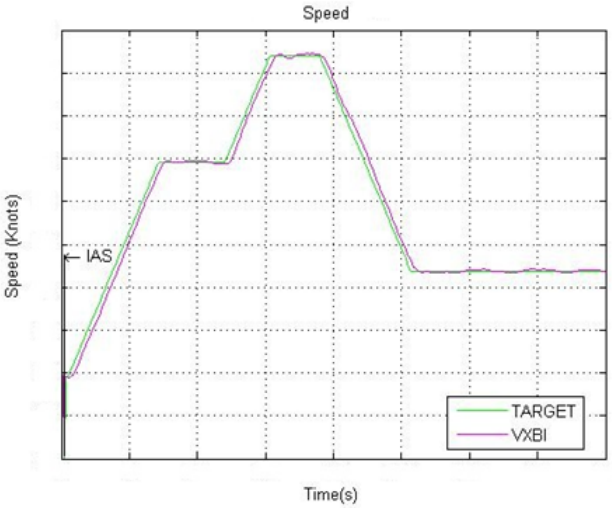

(c)

Figure 6.8: VXBI response to turbulence with cut-off frequency of the velocity filter reducing at each graph

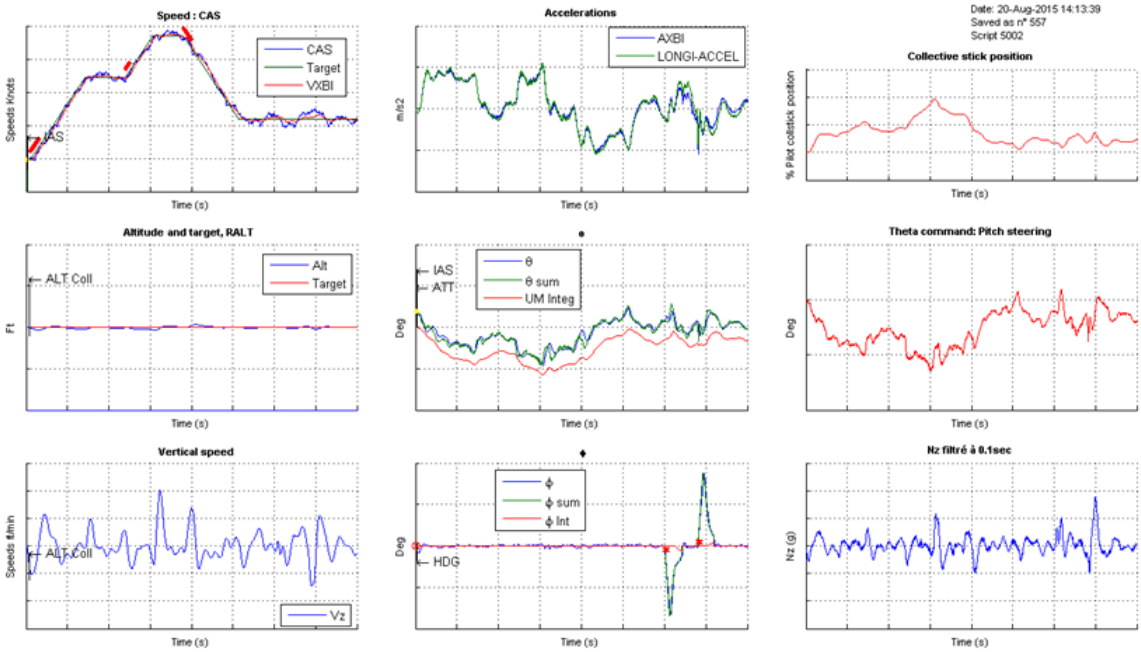

Figure 6.9: Helicopter response in turbulent air with the modified filter

6.2 Turbulence detection mechanism

If one can detect perfectly turbulence occurrences, one can always have a controller more leaned to comfort issue in turbulent air.

The turbulence detection mechanism proposed is based on the statistic parameter, Root Mean Square (RMS). The RMS value of a set of values is the square root of the arithmetic mean of the squares of the values. In the case of a set of n samples $x_1, x_2, .., x_n$, the RMS value of the set is defined by equation 6.1.

$$x_{rms} = \sqrt{\frac{1}{n}(x_1^2 + x_2^2 + ... + x_n^2)} \tag{6.1}$$

The corresponding formula for a continuous function defined over the interval $T_1 \leq t \leq T_2$ is given by equation 6.2.

$$f_{rms} = \sqrt{\frac{1}{T_2 - T_1}\int_{T_1}^{T_2} [f(t)]^2 dt} \tag{6.2}$$

The RMS of the pairwise differences of the two data sets, one from the theoretical prediction of a physical variable and another one from the actual measurement of this variable, can serve to measure how far the average error is from zero. Therefore, assuming the velocity reference as the theoretical prediction of CAS output, the RMS of the difference between the velocity reference and the actual measurement of CAS could be a criterion to measure how far the average velocity error is from 0.

By observing the helicopter behavior in turbulence, an evident characteristic is constant airspeed changes, so it should origin a bigger RMS velocity error than in calm air, figure 6.10 and figure 6.11. However, this fact is only correct when the airspeed is hold without any maneuvers. Operations like speeding up or down the helicopter create a constant velocity shift with respect to the reference due to the delay (see figure 6.12); turning right or left causes the CAS to deviate from the selected velocity and it takes some seconds to converge (see figure 6.13). Therefore, maneuvers can create significant RMS velocity error in calm air, which cannot be distinguished from those caused by turbulence.

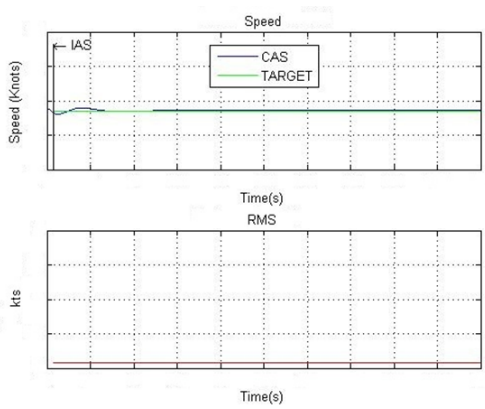

Figure 6.10: Speed response and RMS velocity error in calm air

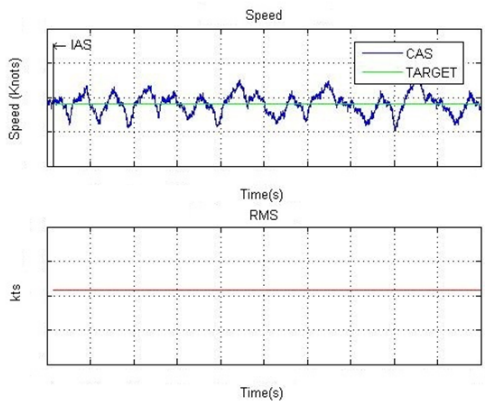

Figure 6.11: Speed response and RMS velocity error in turbulent air

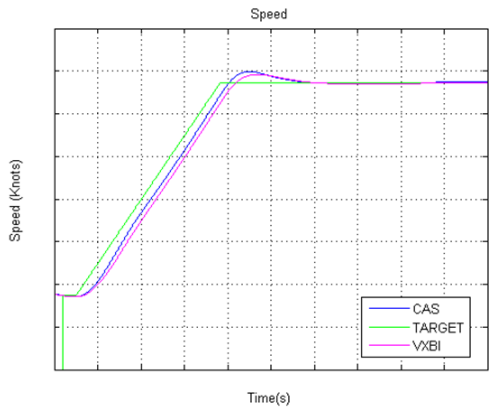

Figure 6.12: Speed response when performing velocity reference change in calm air

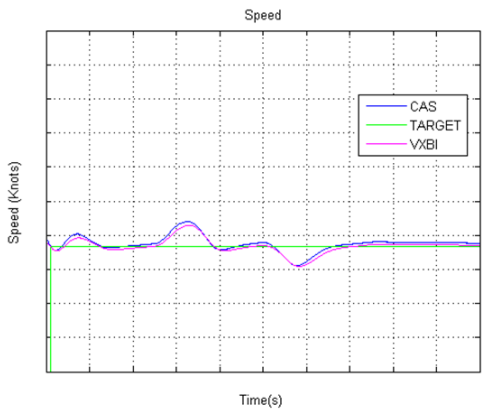

Figure 6.13: Speed response when performing a turn in calm air

The RMS of velocity error during a period of time can be computed by using equation 6.3, where the T is fixed to 10 seconds in order to compute the RMS of velocity error of the last 10 seconds at each instant t.

$$RMS(t) = \sqrt{\frac{1}{T}\int_{t-T}^{t}[(V_{ref} - CAS]^2 dt} \tag{6.3}$$

At first, the RMS method was implemented in the AFCS model to analyze the evolution of RMS of velocity error in calm air and turbulent air. The simulation was performed in airspeed hold condition without any maneuvers. Figure 6.14 shows the variation of RMS error with respect to different levels of turbulence and airspeed, in which the helicopter is flying. It can be seen that the velocity deviation depends on the turbulence level as well as the helicopter airspeed. As expected, one can observe bigger difference between calm and turbulent environment, as the turbulence level augments.

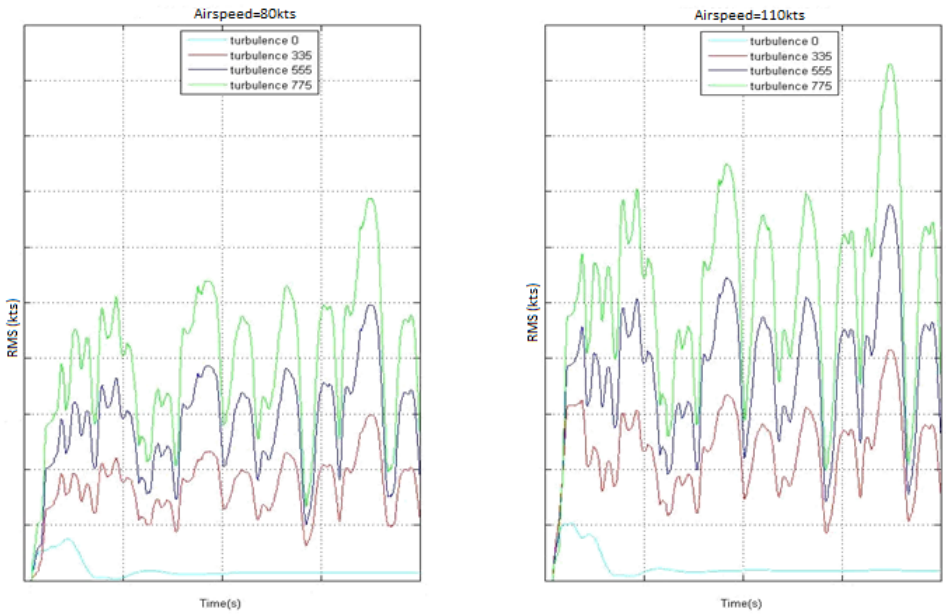

Figure 6.14: RMS error with respect to different levels of turbulence, altitude and airspeed

Small turbulence levels have not much impact on passengers comfort and it is preferable to select the original tuning for use in calm air. Hereby, it is necessary to define a limit above which RMS error it should be considered as turbulent condition, in order to select the desired controller. However, the RMS of velocity error has an oscillatory behavior and a single constant value could not serve the purpose; constant changes in turbulence detection could take place if the RMS of velocity error oscillates around the value defined as frontier between calm side and turbulent side. Therefore, two limits of RMS error are defined, the upper limit and the lower limit. Any RMS greater than the upper limit leads to turbulence detection, and any RMS lower than the lower limit switches off the detection. Any RMS error falling into the region between these two limits has no influence on the detection mechanism. In other words, when the turbulence detection is true, it changes from true to false only when the RMS error reaches a value lower than the lower limit. Likewise, the turbulence detection changes from false to true, only when the RMS overtakes the upper limit.

The RMS method mentioned above requires the velocity reference, which is only available when a speed hold mode like IAS is engaged. Therefore, the mechanism can only be applied during speed hold condition. Moreover, as mentioned earlier, maneuvers cause airspeed deviation with respect to the target in calm air, which can mislead to turbulence detection. Therefore, the RMS error method cannot be used to detect turbulence when a maneuver occurs. Logic operators can be included to deactivate the detection mechanism in maneuver conditions.

The turbulence block, which includes RMS velocity error calculation and activation mechanism, was added to switch the speed controller. Figure 6.15 shows the behavior of the turbulence detection mechanism in

calm air and turbulent air. At the beginning, where the velocity change is performed, the RMS calculation is not activated; therefore the detection is false in both calm and turbulent air. When the airspeed is hold, the RMS velocity error is computed and compared to the RMS limits at each instant. As shown in the graphics, turbulence is detected in turbulent air, while the detection of turbulence is always false in calm air. When the detection is true, the mechanism changes the controller to the more damped one for comfort issue. In the case presented, the alternative filter is included in the AFCS for operating in turbulent air. It can be seen in the figure, when turbulence is detected, the behavior of the VXBI changes due to the selection of the alternative filter by the turbulence detection mechanism.

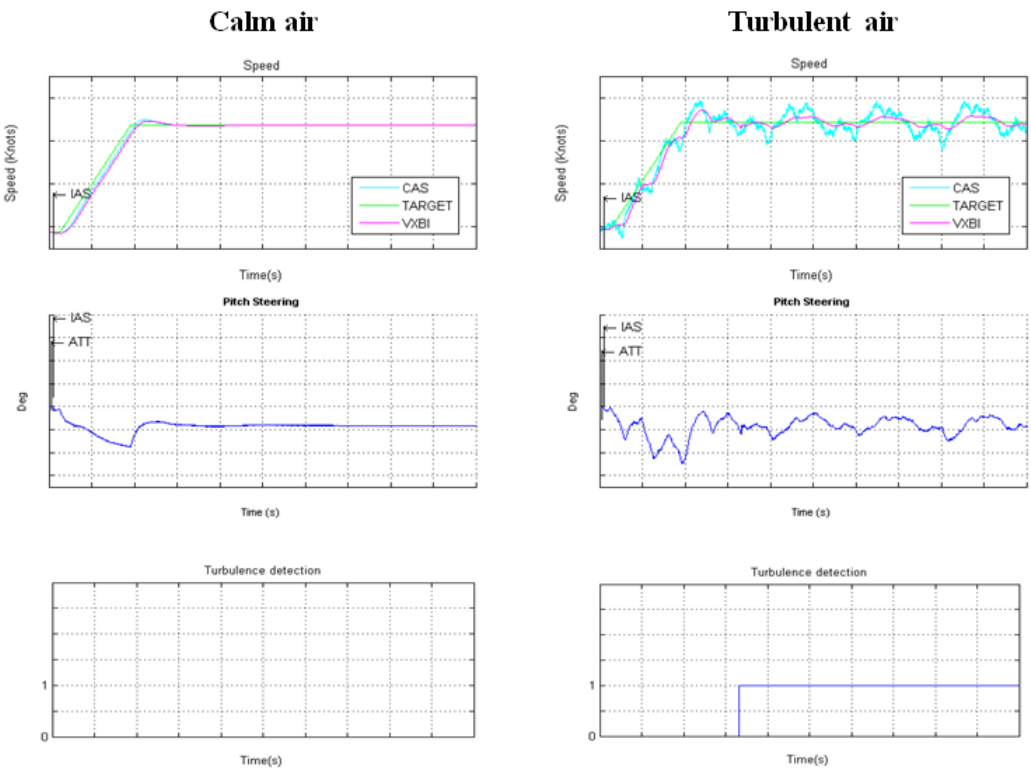

Figure 6.15: Response of the turbulence detection mechanism in calm air and turbulent air

6.3 Performance evaluation of modified filter

Since developing a turbulence detection mechanism is very difficult task due to the random behavior of turbulence, one has thought to evaluate the possibility of using the improved filter all the time.

Unlike a control law gains reduction, it seems possible to keep a reactive control law by using the improved filter. Therefore if the loss in performance is admissible, one can use this modified filter continually in either turbulent or calm environment. The airspeed performance given by the modified filter is analysed in two different maneuvers condition:

1. Speed hold with airspeed reference change (mode IAS, ALT engaged)
2. Speed hold while performing a climb (mode IAS, VS engaged)

First of all, the airspeed performance given by the modified filter in calm air is studied. The response of the helicopter to the first maneuver condition, airspeed reference change, is presented in figure 6.16. The airspeed performance given by the modified filter is compared to the one given by the original filter, in

figure 6.17. One can observe that the response of CAS in order to track the velocity target is nearly the same in both cases. The other maneuver, the change of vertical speed reference, is presented in figure 6.18. In figure 6.19, the airspeed diverges slightly from the target during the maneuver, and this small deviation converges quickly to the reference, with either the original filter or the new one. In summary, in calm air, the airspeed performance given by the modified filter is as good as the one given by the original filter.

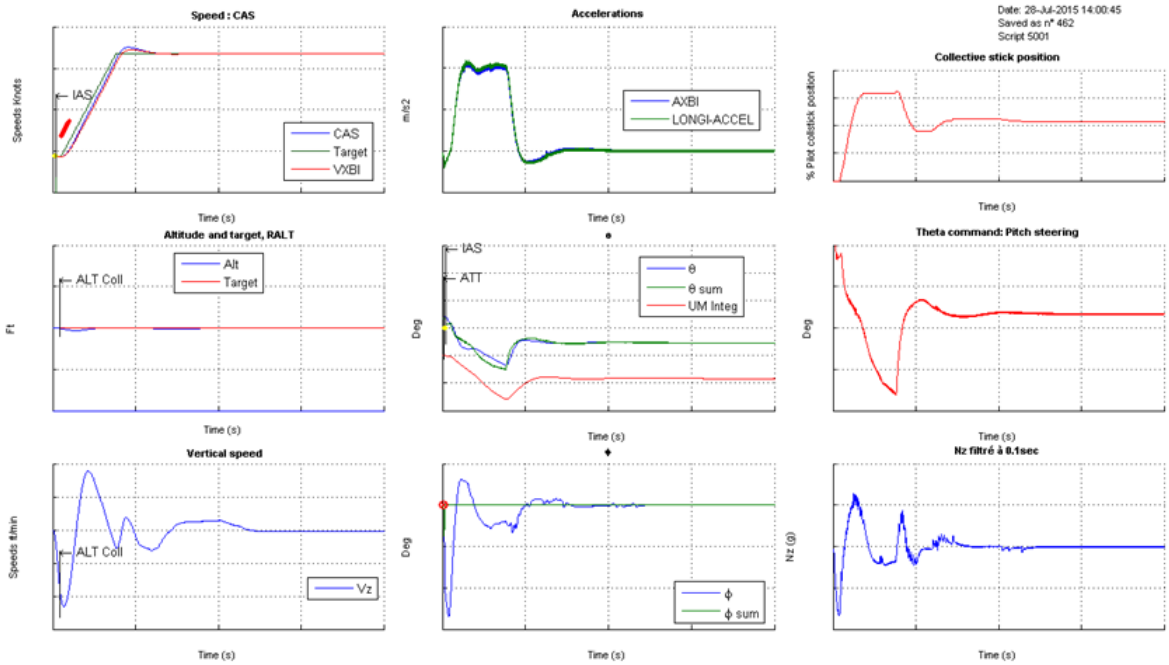

Figure 6.16: Speed hold with airspeed reference change (mode IAS, ALT engaged) in calm air

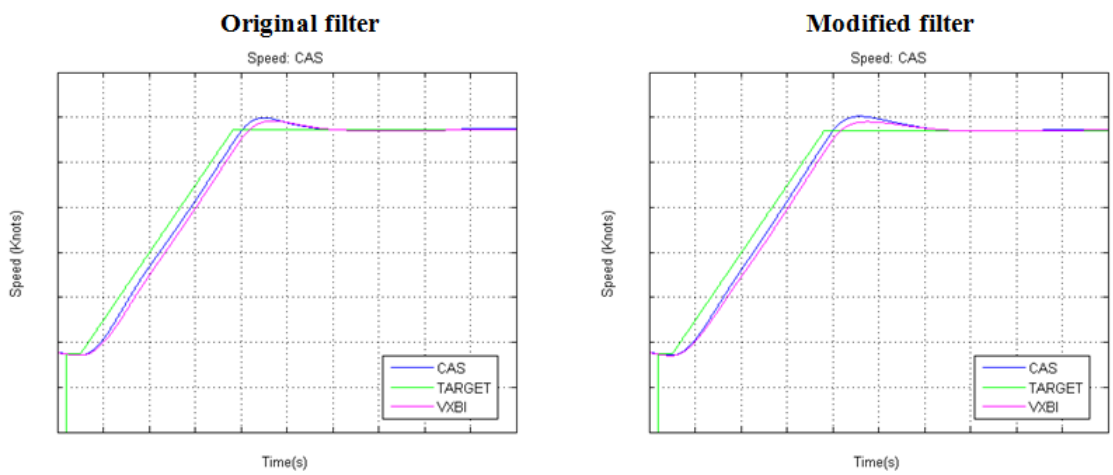

Figure 6.17: Speed response to airspeed reference change

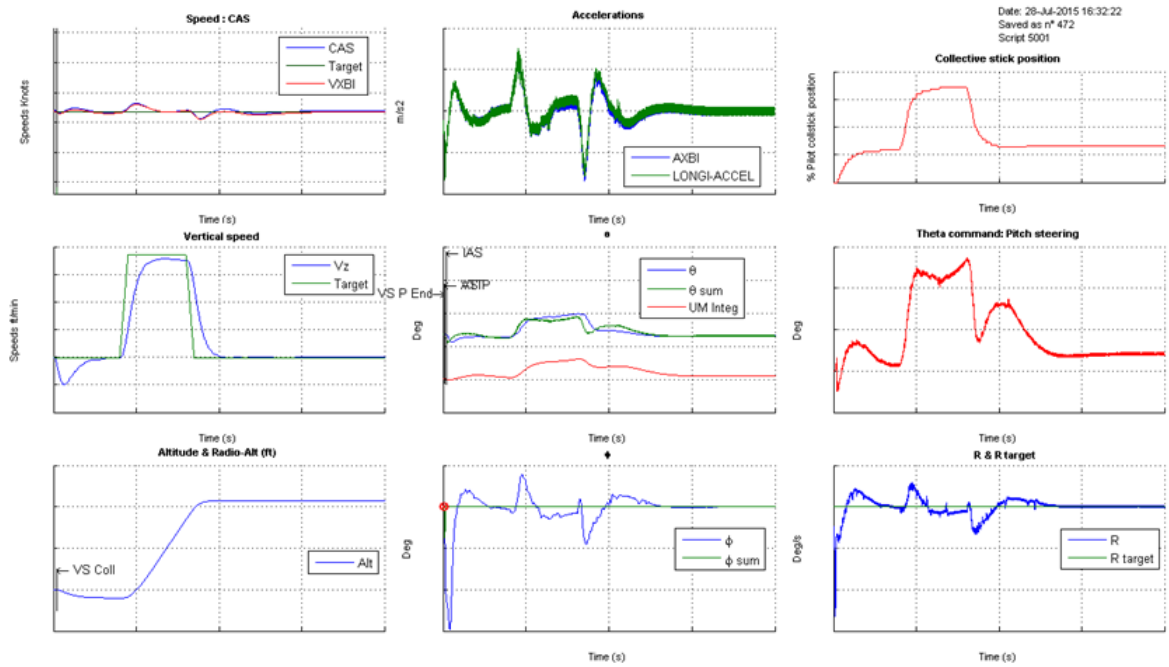

Figure 6.18: Speed hold while performing a climb (mode IAS, VS engaged) in calm air

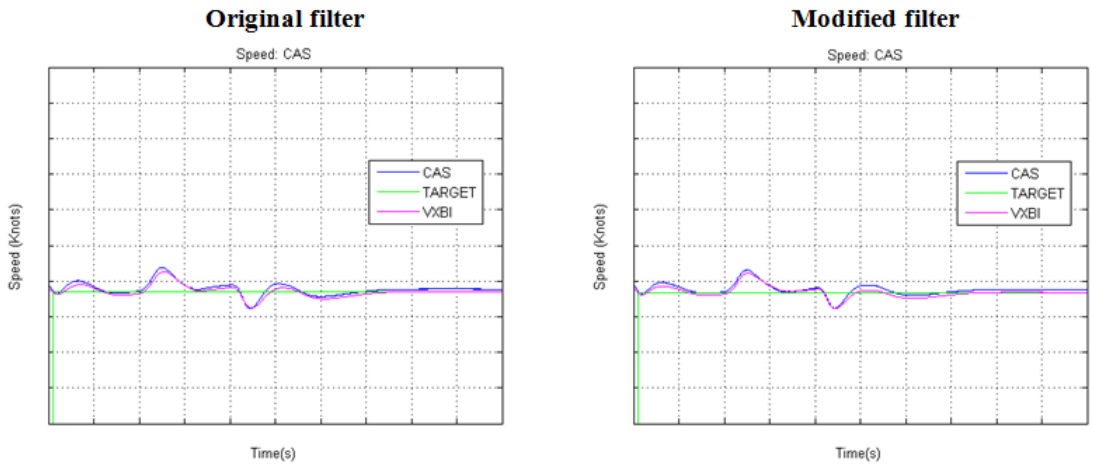

Figure 6.19: Speed response to vertical speed reference change

In the presence of turbulence, the velocity deviation from the reference is inevitable. In spite of the improvement achieved by the modified filter in terms of acceleration changes, the consequence on the airspeed performance should be analysed.

Concerning the speed performance in a turbulent environment, the RMS velocity error is used to evaluate the performance of the improved filter with respect to the original filter. In both maneuver conditions, the results did not show evident drawbacks (figure 6.20 and figure 6.21). There is no significant difference in airspeed deviation between using the original filter and the modified filter. The RMS errors are practically the same, even when maneuvers are performed.

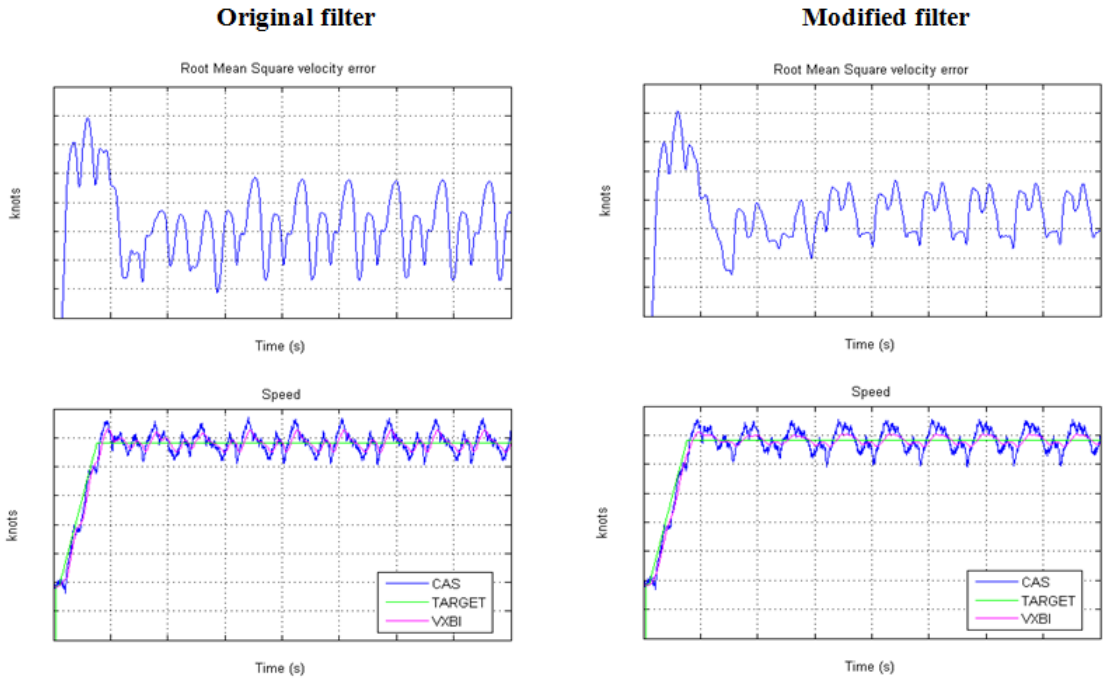

Figure 6.20: Speed hold with airspeed reference change (mode IAS, ALT engaged) in turbulent air

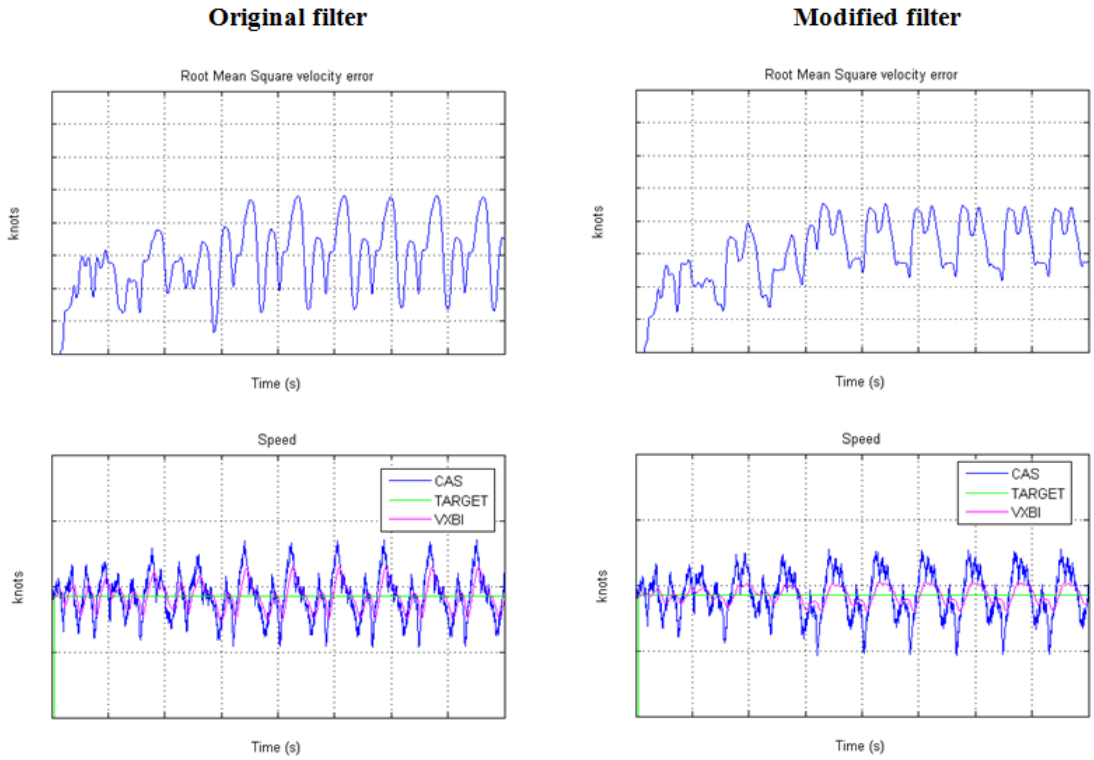

Figure 6.21: Speed hold while performing a climb (mode IAS, ALT engaged) in turbulent air

6.4 Comfort evaluation

The comfort criterion, described previously in the bibliographic research section, is applied to evaluate passengers comfort in turbulent air. The objective is to compare the comfort given by the original filter and the modified filter.

Several simulations were performed by introducing different turbulence conditions. Here, only results from two simulation cases are discussed. First simulation includes bigger turbulence length than the second simulation, which means that the turbulence frequency is increased in the second simulation case.

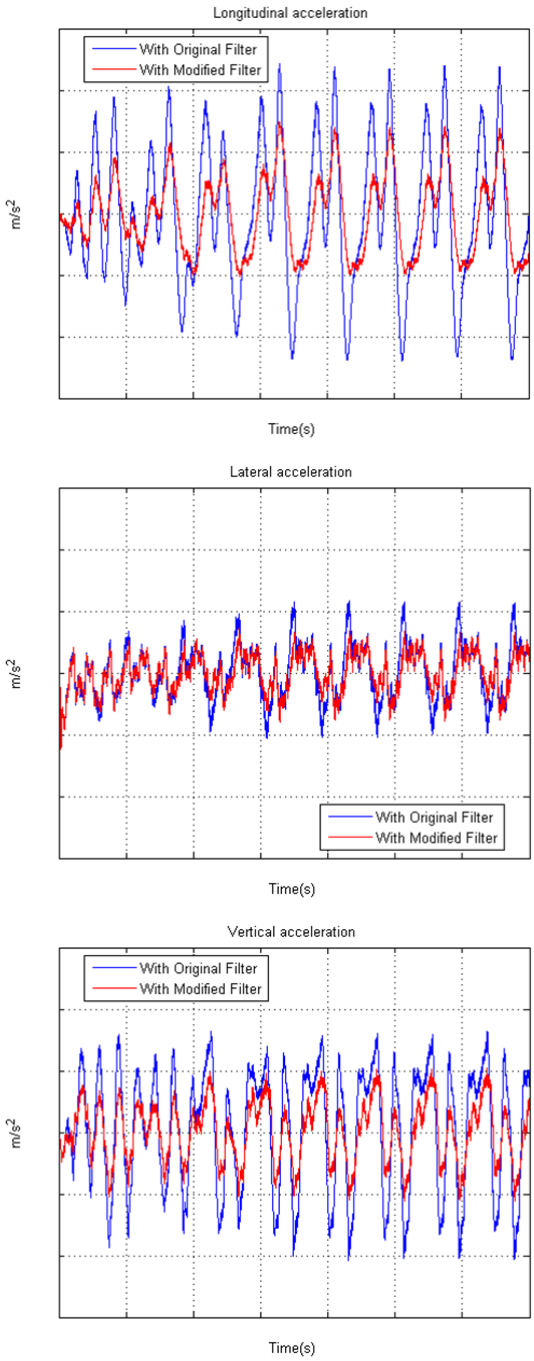

Figure 6.22

As described in the section 5.2, in order to evaluate "low frequency" comfort (vibrating comfort) and "very low frequency" comfort (motion sickness), the accelerations have to be measured at the pilot position to calculate the total vibration value a_v, equation 5.4, and PIP, equation 5.7. As the position of the sensor AHRS is close to the pilot position, the accelerations measured by AHRS are used. The acceleration responses from AHRS with original filter and modified filter for the same flight conditions are shown in figure 6.22.

After obtaining the measured accelerations, the frequency weighting curves have to be applied to the measured accelerations to obtain the frequency weighted accelerations. The documentation [13] presents the low order filter approximations of the frequency weighting curves, which are used to obtain frequency weighted acceleration.

Concerning "low frequency" comfort (vibrating comfort), a fifth order filter $W_k^{(5)}(s)$ is used for weighting vertical acceleration and a fourth order filter $W_d^{(4)}(s)$ is used for weighting horizontal acceleration. The filter $W_k^{(5)}(s)$ and $W_d^{(4)}(s)$ are represented respectively by the equation 6.4 and equation 6.5, according to [13]; their correspondent magnitude frequency responses are exposed in figure 6.23 and figure 6.24.

$$W_k^{(5)}(s) = \frac{87.72s^4 + 1138s^3 + 11336s^2 + 5453s + 5509}{s^5 + 92.6854s^4 + 2549.83s^3 + 25969s^2 + 81057s + 79783} \tag{6.4}$$

$$W_d^{(4)}(s) = \frac{12.66s^3 + 163.7s^2 + 60.64s + 12.79}{s^4 + 23.77s^3 + 236.1s^2 + 692.8s + 983.4} \tag{6.5}$$

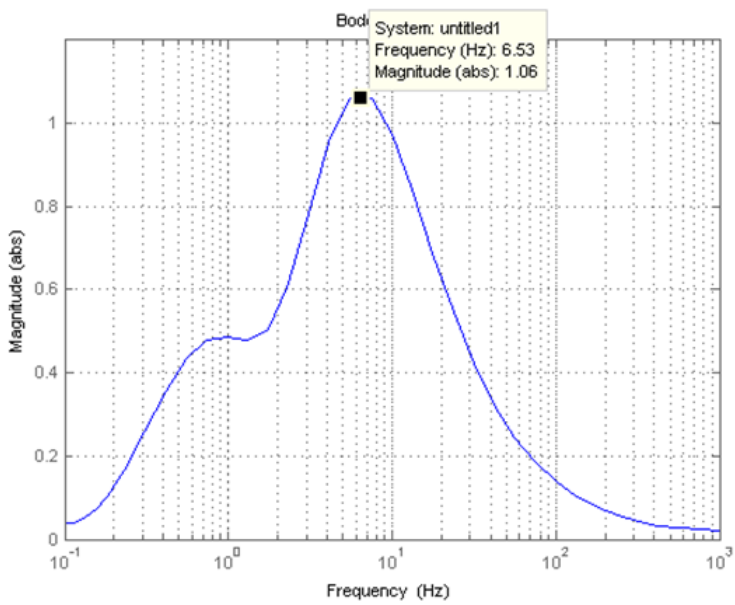

Figure 6.23: Magnitude frequency response of $W_k^{(5)}(s)$

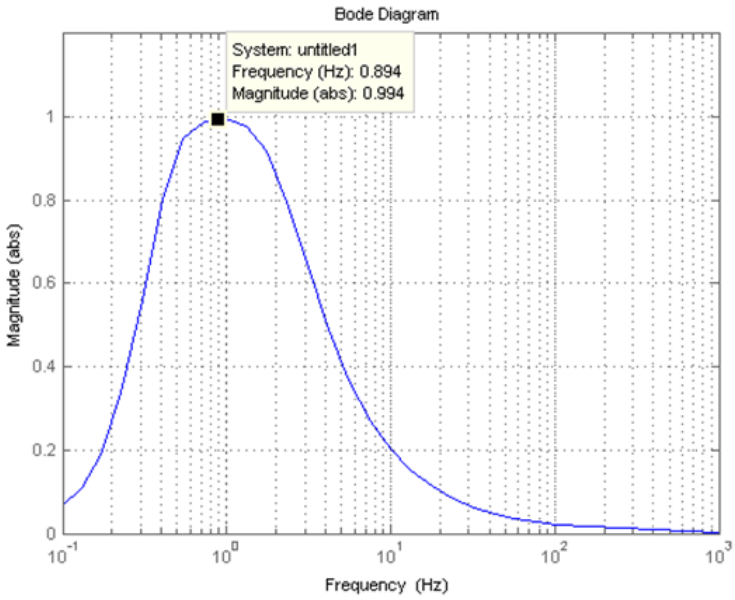

Figure 6.24: Magnitude frequency response of $W_d^{(4)}(s)$

The overall weighted acceleration at the AHRS position is computed by using the equation 5.4 and the results are shown in table 6.1. The value of a_v is small with either the original filter or the modified filter. As the values of a_v are less than 0.315 m/s^2, the (dis)comfort category is "not uncomfortable" according to the table presented previously in figure 5.6.

Table 6.1: RMS values of weighted accelerations (a_{wx}, a_{wy}, a_{wz}) and total vibration (a_v) obtained for the original filter and the modified filter

Filter	$a_{wx}(m/s^2)$	$a_{wy}(m/s^2)$	$a_{wz}(m/s^2)$	$a_v(m/s^2)$
Original	0.0209	0.0356	0.0328	0.0527
Modified	0.0152	0.0318	0.0218	0.0414

As already mentioned, the critical frequencies for "vibrating comfort" are 1 Hz for the horizontal acceleration and between 4 to 8 Hz for vertical ones. In order to study the impact of the modified filter in acceleration responses at these critical frequencies, the measured accelerations are analysed in the frequency domain. This study in the frequency domain can also provide information about at which frequencies accelerations are affected by turbulence. Figure 6.25 shows the acceleration response in frequency domain and the results point out that the turbulence mainly affects frequencies lower than 0.1Hz, which are far from the critical frequencies of human response to vibration. The modified filter improves the response at frequencies lower than 0.1Hz. Indeed, at these frequencies, an evident reduction of the amplitude is noted with the modified filter. The effect of turbulence on the critical frequencies for "vibrating comfort" is little, which confirms the small values of a_v in table 6.1.

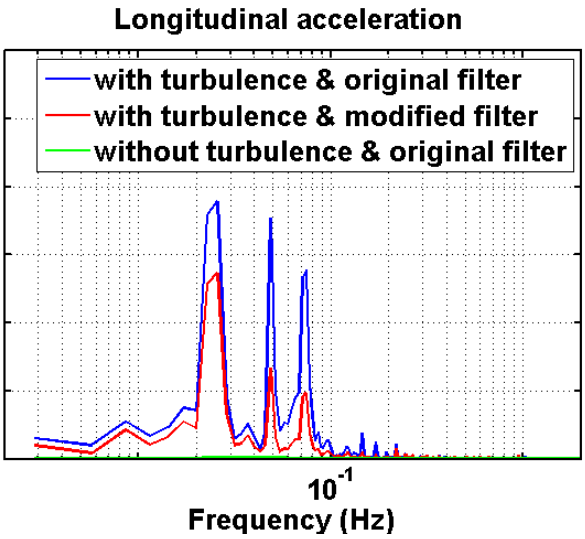

(a)

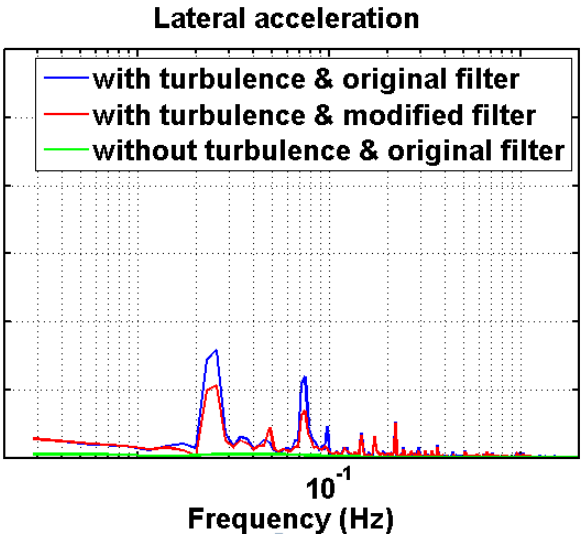

(b)

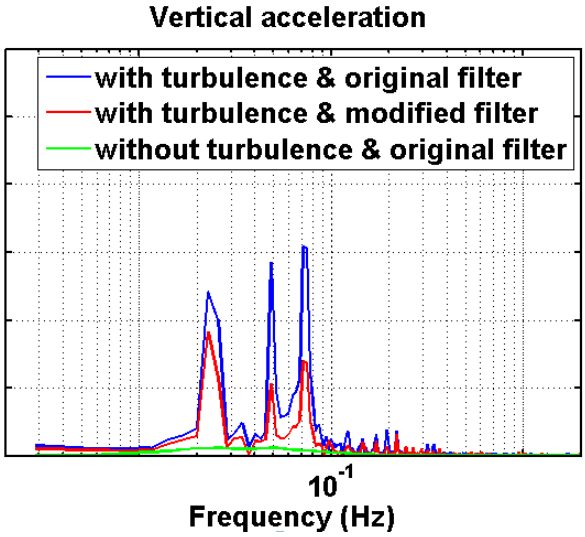

(c)

Figure 6.25: Frequency response of the measured accelerations

Regarding "very low frequency" comfort (motion sickness phenomenon), the weighting filter applied to the accelerations is a fifth order approximation $W_f^{(5)}(s)$, which is represented by equation 6.6 from [13]. Its magnitude frequency response is presented in figure 6.26, where the critical frequencies for the motion sickness phenomenon are located near to 0.17Hz. The specifications defined in ISO 2631-1 for motion sickness are only given for vertical axis. However, it is considered here that the specifications are also applicable to longitudinal and lateral axis.

$$W_f^{(5)}(s) = \frac{0.1457s^4 + 0.2331s^3 + 13.75s^2 + 1.705s + 0.3596}{s^5 + 7.757s^4 + 19.06s^3 + 28.37s^2 + 18.52s + 7.230} \tag{6.6}$$

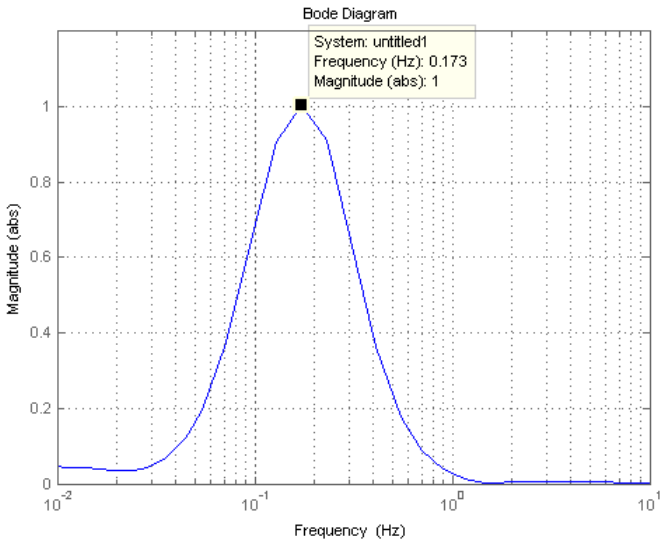

Figure 6.26: Magnitude frequency response of $W_f^{(5)}(s)$

Table 6.2 presents the PIP obtained for the original filter and the modified filter.

Table 6.2: PIP obtained for the original filter and the modified filter

Filter	PIP longitudinal (%)	PIP lateral (%)	PIP vertical (%)
Original	0.85	0.51	0.97
Modified	0.30	0.41	0.48

It can be seen in figure 6.25, the effect of turbulence on the accelerations at frequencies of motion sickness is small, however, the amplitude of the longitudinal and vertical accelerations at these frequencies is slightly reduced with the modified filter. Table 6.2 evidences the reduction of PIP with the modified filter.

The second flight simulation case in turbulent air is performed with bigger frequency of turbulence (smaller turbulence scale length). The acceleration responses in the time domain with original filter and modified filter are shown in figure 6.27. The acceleration responses in the frequency domain with original filter and modified filter are shown in figure 6.28.

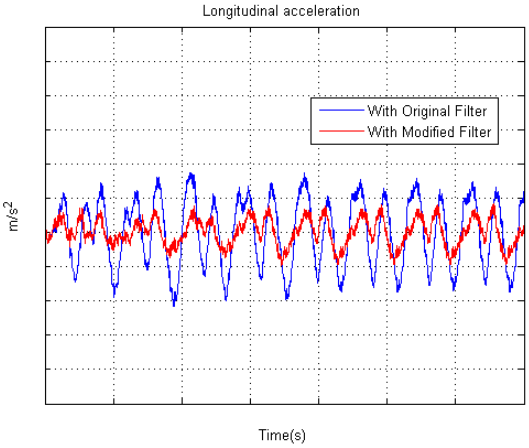

(a)

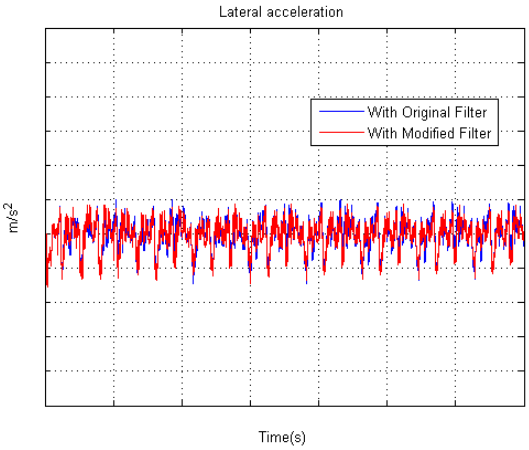

(b)

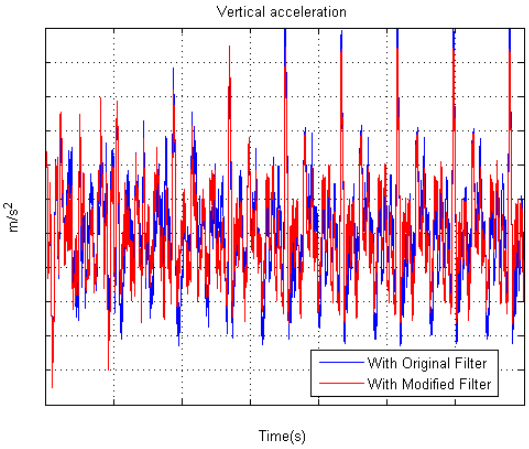

(c)

Figure 6.27: Time response of the measured accelerations

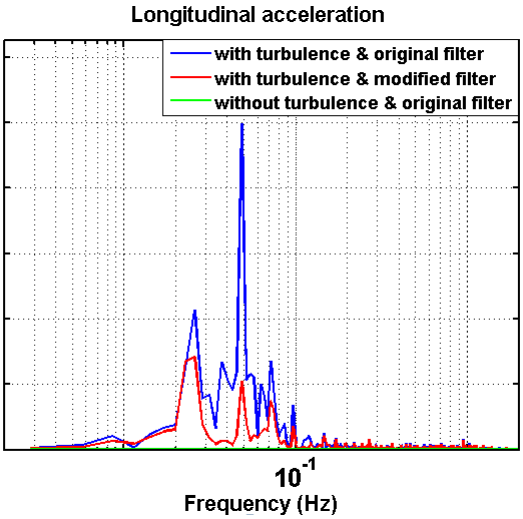

(a)

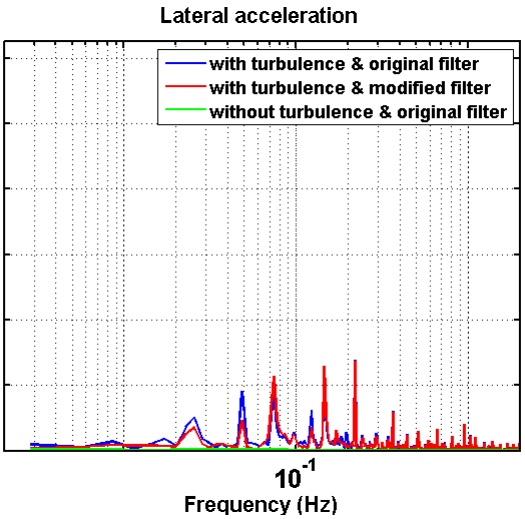

(b)

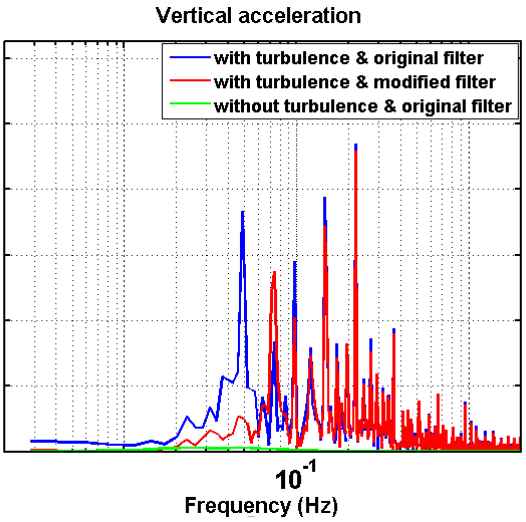

(c)

Figure 6.28: Frequency response of the measured accelerations

For longitudinal acceleration, figure 6.28 shows that the turbulence affects mainly frequencies lower than 0.1Hz and the modified filter reduces always the amplitude of accelerations at these frequencies. For lateral and vertical accelerations, the main frequencies affected by turbulence include the critical frequencies of motion sickness phenomenon and, the modified filter does not improve the acceleration responses at these frequencies. The PIP values for lateral and vertical axis from table 6.3 confirms the fact mentioned.

Table 6.3: PIP obtained for the original filter and the modified filter

Filter	PIP longitudinal (%)	PIP lateral (%)	PIP vertical (%)
Original	1.2	1.9	7.4
Modified	0.6	1.9	7.1

One should take into account that the values a_v and PIP depend on the turbulence intensity and frequency. In addition, the standard was derived from seaboard studies and the motion sickness phenomenon is evaluated for the vertical axis. In this study, the specifications for the vertical axis were applied to the longitudinal and lateral axes.

Summarizing, the comfort criterion was applied to a flight simulation case for two different turbulence frequencies. For the longitudinal acceleration, turbulence mainly affects frequencies lower than 0.1Hz in both simulation cases. It seems that the frequencies of longitudinal acceleration affected by turbulence don't change with the turbulence frequency. However, the results indicate that the maximum amplitude of accelerations increases when the turbulence has higher frequency. For the lateral and vertical axes, accelerations of higher frequencies are detected when the frequency of turbulence is increased. Also, the maximum amplitude of lateral and vertical acceleration is increased with a bigger turbulence frequency.

In terms of improvement by using modified filter, it can be seen that the longitudinal acceleration is always reduced. However, the lateral and vertical acceleration responses are not always improved with the modified filter. It is logical because the modification on the filter aims to reduce longitudinal accelerations.

Even though, the comfort criterion is not derived for helicopter flight studies and the critical frequencies for comfort evaluation are unknown, the amplitude of longitudinal acceleration is always reduced with modified filter in the cases considered. One should also take into account that all the results are obtained with the turbulence model defined in the documentation [9].

7 Evaluation with flight test data

Although simulation environments and computer capabilities have evolved enormously, it is not possible to reproduce in simulation the unpredictability of reality. Previous results concerning the behavior of the modified filter and the turbulence detection were obtained from the simulation, which don't represent completely the reality. This section intends to evaluate the modified filter and the turbulence detection mechanism in the real flight conditions, with help of flight test data. The first section is dedicated to the verification of the new filter behavior, in a turbulent flight test case. In the second section, the turbulence detection mechanism is evaluated, in a turbulent air flight and calm air flight.

7.1 Verification of simulated VXBI

In this first section, a flight test data in turbulent air is used to evaluate the modified filter behavior towards realistic flight conditions. Figure 7.1 exposes the helicopter responses of the flight case.

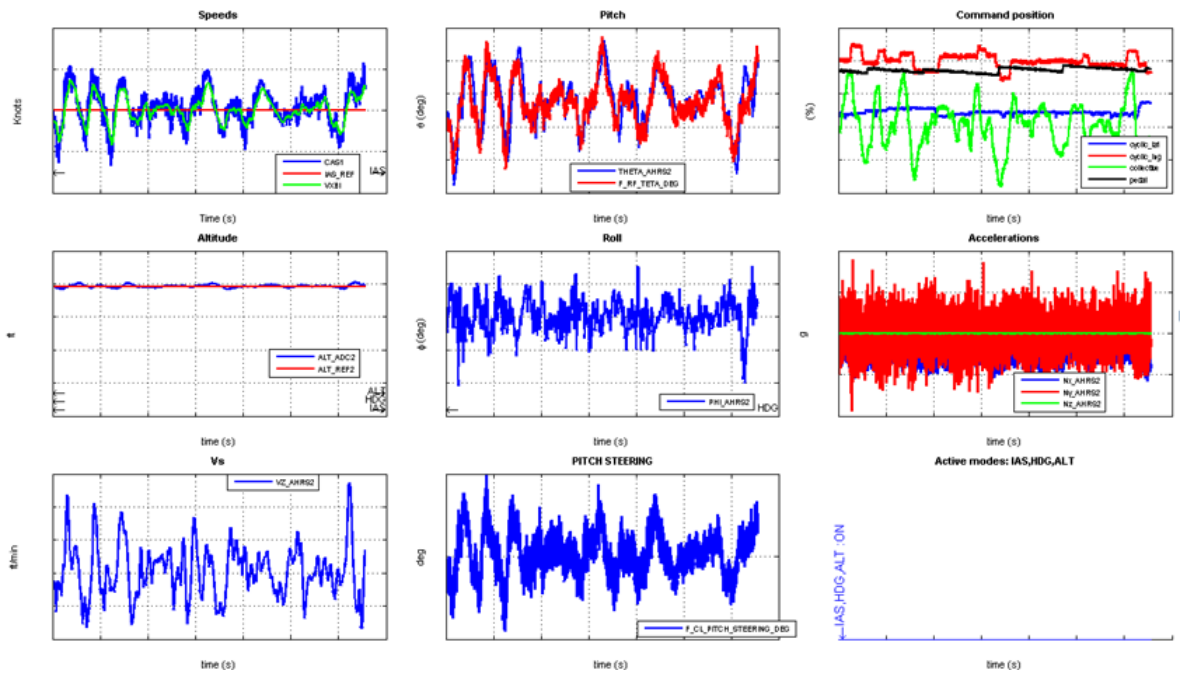

Figure 7.1: Helicopter response in turbulent air from flight test data

First, the verification of the simulation is performed. The filter block presented earlier is used to generate a "simulated VXBI", by using the airspeed and inertial acceleration from flight test data. Then, the "simulated VXBI" is compared to the VXBI from the flight test data, in order to verify the match between them, when using the same tuning. The left graphic of figure 7.2 confirms the match between

the two VXBI. Once the filter block is verified, the improvement of VXBI behavior by using the modified filter should be analysed. However, one can only evaluate this last point with open loop. The right graphic of figure 7.2 indicates that the new VXBI has a smoother response compared to the original one, which has a similar response to the one obtained from the closed-loop simulations.

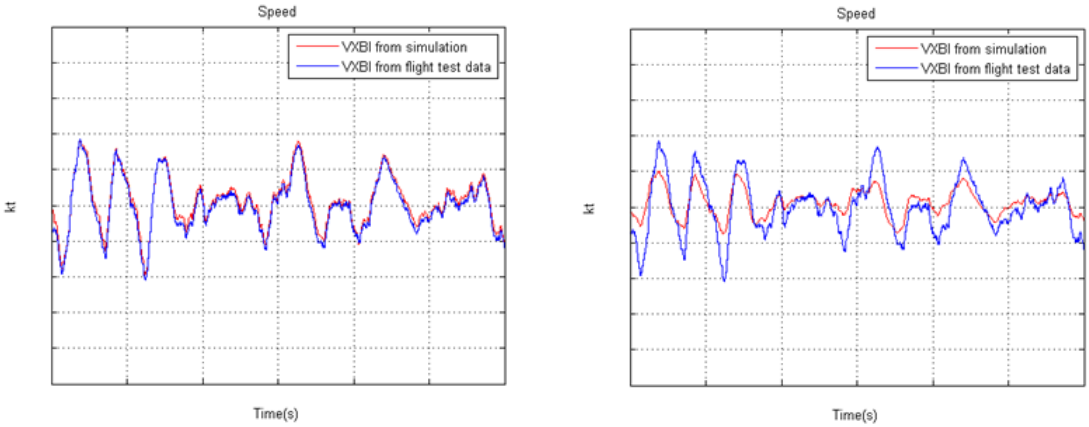

(a) Original filter

(b) Modified filter

Figure 7.2: VXBI response by using flight test data

7.2 Comparison of detection mechanism without and with turbulence

The results from section 6.2 showed evident difference between the RMS from turbulent air and the one from calm air. The value of activation and deactivation were defined according to the results from the simulation. However, these results were obtained from the simulation where no disturbances were included in the "0 level" turbulence, perfect calm condition was performed. As a matter of fact, perturbations are always present, even in calm air. In addition, the turbulence simulated has practically constant behavior that repeats over time.

In order to evaluate the turbulence detection mechanism in a realistic random turbulence and calm conditions, flight test data was used. The turbulent flight case used is the one presented previously in the verification of VXBI (figure 7.1). The flight case in a calm environment is presented in figure 7.3, where the helicopter is flying with IAS mode engaged as well.

In order to calculate the RMS of velocity error, CAS and velocity reference from the flight cases are used. Figure 7.4 shows the RMS evolution calculated in the turbulent air flight and calm air flight, where T was considered equal to 10 seconds, the same one defined in the simulation. If the upper limit and lower limit to activate and deactivate defined earlier in the simulation are applied in the turbulent flight test case, the detection mechanism would experience constant changes and it does not remain active as expected. The undesirable deactivation can be avoided if the lower limit is reduced. However, the value will be too small and there will be difficulties in detecting calm air, once the condition in which the helicopter was flying changes from turbulent to calm.

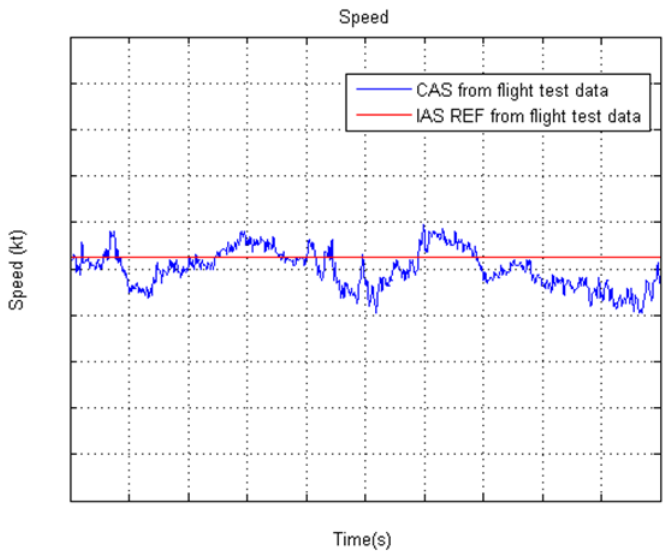

Figure 7.3: Speed response in calm air from flight test data

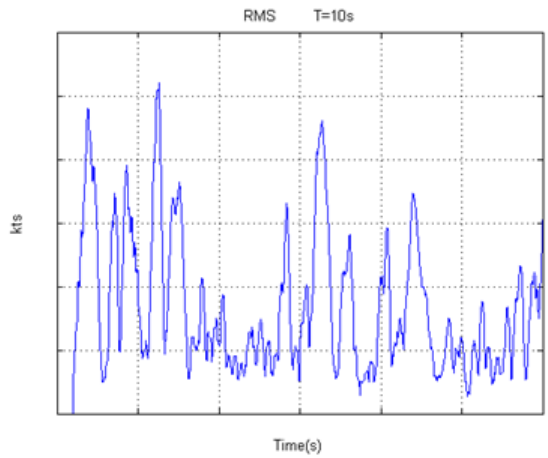

(a) Turbulent air flight case

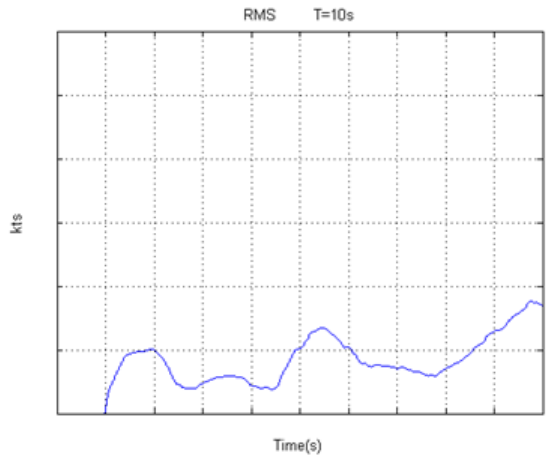

(b) Calm air flight case

Figure 7.4: RMS of velocity error with T=10s

Excessive amplitude changes of the RMS signal is due to the small period of RMS calculation, T. Using a longer period for computing RMS would give RMS values closer to the average. Figure 7.5 shows the evolution of the RMS calculated for T equals to 50 seconds instead of 10 seconds. As one can observe, both variation of RMS in turbulent flight or calm flight are smoother. However, by a using bigger T, it requires more data storage for RMS calculation and, the activation takes a longer time to happen, when the helicopter encounters the turbulence.

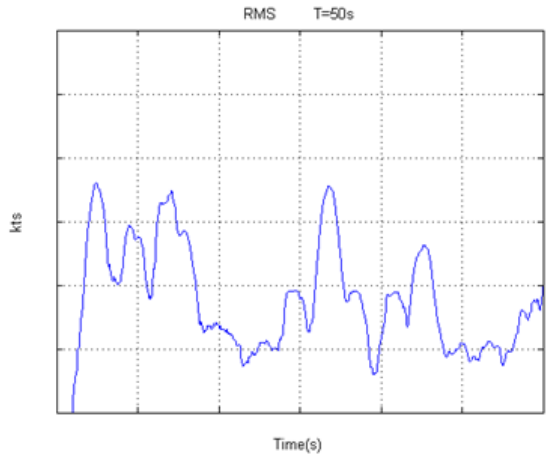

(a) Turbulent air flight test case

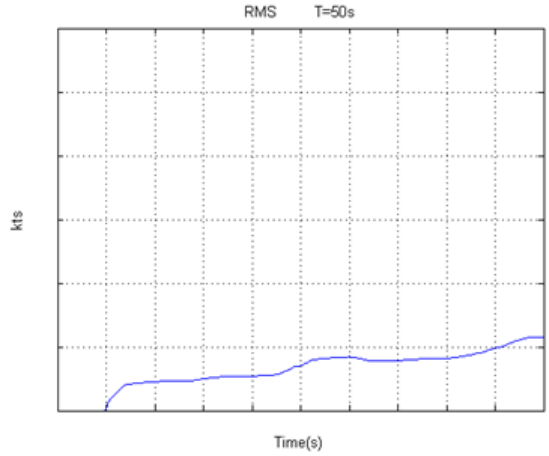

(b) Calm air flight test case

Figure 7.5: RMS of velocity error with T=50s

The alternative solution to avoid the constant activation and deactivation is to filter the RMS values in order to eliminate excessive changes during the time. In addition, confirmation logic can be added to avoid instantaneous RMS falling below the lower limit, while the helicopter is still surrounded by turbulent air.

The low pass filter is implemented after the RMS computation in the simulation. In order to analyze the behavior of the filter, the RMS were calculated without filter during 50 seconds to compare the evolution between this and the one calculated with filter and T equals to 10 seconds. Figure 7.6 and figure 7.7 illustrate the RMS signal using the filter oscillates nearly around the value when using longer period of calculation.

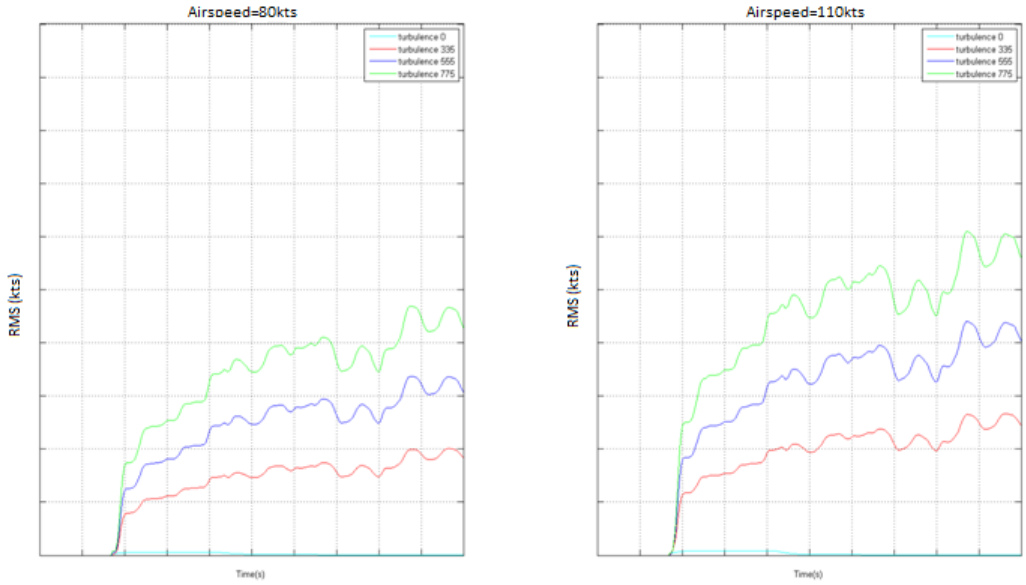

Figure 7.6: RMS of velocity error with T=50s from the simulation

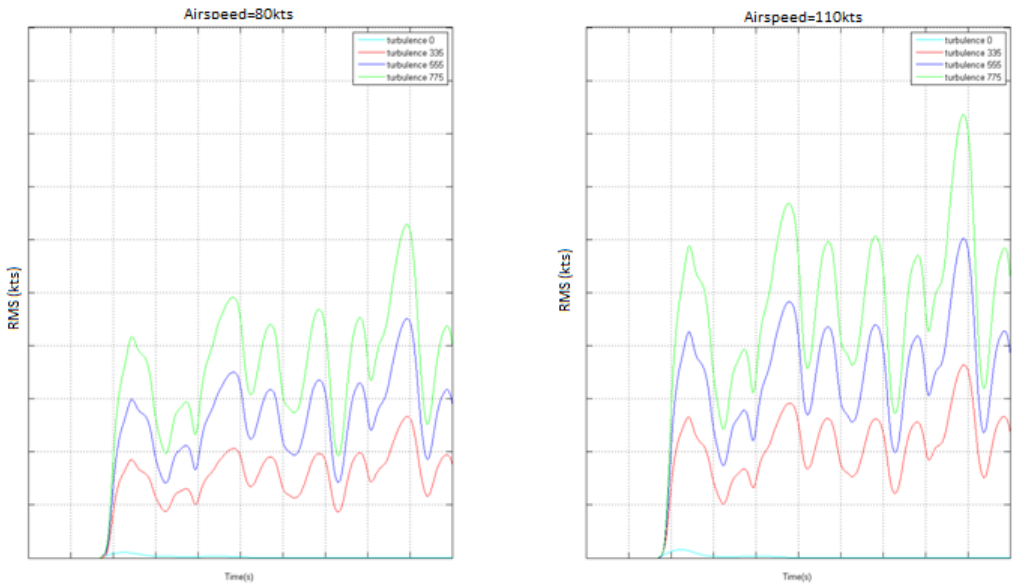

Figure 7.7: RMS of velocity error with T=10s and a low pass filter from the simulation

In the end, the filter is applied to calculate RMS with flight test data and, the confirmation logic is added alongside with the detection logic. Figure 7.8 presents the results for turbulent flight case and calm flight case. The curves of blue color are the RMS values and curves of red color are RMS limits for activation and deactivation. In both cases, the turbulence detection mechanism achieved what as intended; turbulence is detected all the time in the turbulent flight, while the detection of turbulence is always false in the calm flight case.

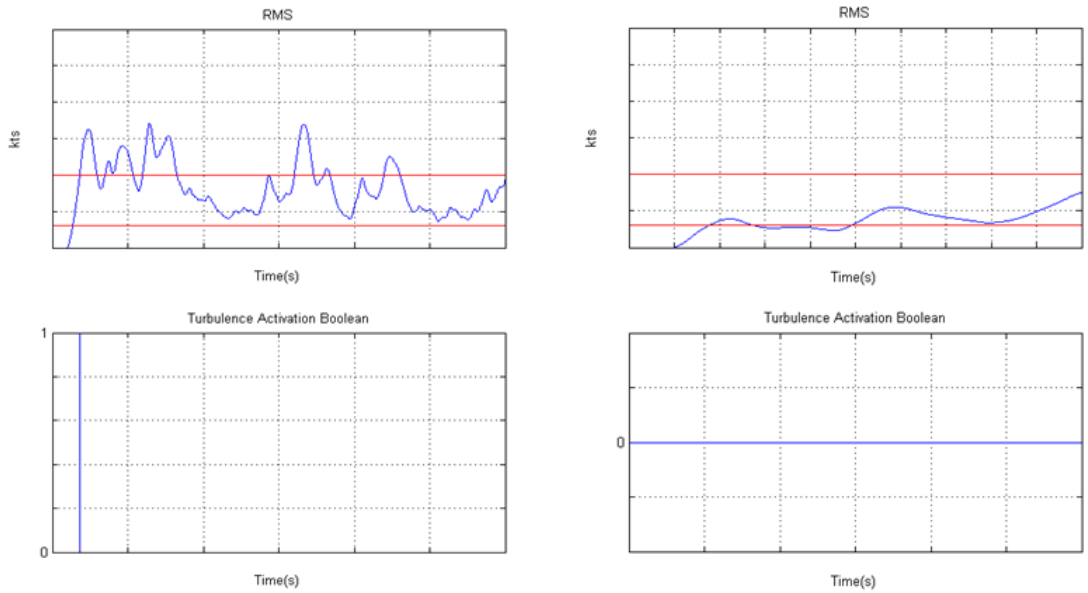

(a) Turbulent air flight test case

(b) Calm air flight test case

Figure 7.8: RMS of velocity error and turbulence detection in calm and turbulent air

8 Conclusions

The reduction of the speed control activity is achieved by using small gains in the control law or by reducing the cut-off frequency in the filter. In both cases, the undesirable acceleration changes, encountered in turbulent air, are less than the ones given by the original speed controller. However, it seems that the approach of the modified filter is more advantageous. The study revealed similar airspeed performance of the modified filter with respect to the original filter, in both calm air and turbulent air. In the future, other factors should be analysed to evaluate the possible consequences of using the modified filter in all conditions.

Detecting turbulence is a difficult task due to its random behavior. The RMS method alongside with the low pass filter and the confirmation logic performed as desired in two flight test cases. However, this first approach for the turbulence detection mechanism has to be analysed under more flight test cases, in order to adjust the activation/deactivation mechanism. In the future, this mechanism should be improved to overcome some limitations.

Bibliography

[1] U.S. Department of Transportation, Federal Aviation Administration, Helicopter Flying Handbook (FAA-H-8083-21A), 2012.

[2] Shawn Coyle, Cyclic and Collective, Lulu. com, 2009.

[3] U.S. Department of Transportation, Federal Aviation Administration, Rotorcraft Flying Handbook (FAA-H-8083-21), 2000.

[4] U.S. Department of Transportation, Federal Aviation Administration, Helicopter Instructor's Handbook (FAA-H-8083-4), 2012.

[5] K. J. Schulte, G. Eldredge, Automatic Velocity Control System For Aircraft, 2011.

[6] C. R. Hanke, Wind Shear Responsive Turbulence Compensated Aircraft Throttle Control System, 1983.

[7] H. Seidel, M. J. Griffin, Whole-Body Vibration, Retrieved on July 9, 2015.

[8] M. A. Bellmann, Perception of Whole-Body Vibrations: From basic experiments to effects of seat and steering-wheel vibrations on the passenger's comfort inside vehicles, Ph.D. thesis, Oldenburg, 2002.

[9] D. J. Moorhouse, R. J. Woodcock, Background Information and User Guide for MIL-F-8785C, Military Specification - Flying Qualities of Piloted Airplanes, Technical Report, AF Wright Aeronautical Laboratories, AFSC, Ohio, 1982.

[10] U.S. Department of Transportation, Federal Aviation Administration, Instrument Procedures Handbook (FAA-H-8083-16A), 2015.

[11] F. Kubica, B. Madelaine, Passenger Comfort Improvement by Integrated Control Law Design, Technical Report, Aerospatiale Matra Airbus, Toulouse, 2000.

[12] A. Lawther, M. J. Griffin, Prediction of the incidence of motion sickness from the magnitude, frequency, and duration of vertical oscillation, The Journal of the Acoustical Society of America 82 (1987) pp. 957–66.

[13] L. Zuo, S. Nayfeh, L. Zuo, S. Nayfeh, Journal Of Sound And Vibration (2002).

A Appendix A

A.1 Company presentation

A.1.1 Thales Group

Our world is increasingly mobile, interconnected and interdependent. Thales believes that in this situation the security of people, goods, infrastructure and nations depends on the ability for leaders and organizations to make the good decisions and act in a timely fashion.

In the markets that Thales serves - defense, security, space, aerospace and ground transportation - these decisions are often of critical importance. The decision makers need full, relevant and reliable information to understand the situation and make the right choices. Thales business lines cover this entire decision chain, from sensors and data gathering to action via secure data transmissions and data processing.

Thales operates in 56 countries with a 2012 revenue of 14 billion euros and a near 1 billion euros EBIT. Thales has a global leadership in many key markets. For example, the group is number one worldwide in payloads for telecoms satellites, air traffic management, sonars and secure transmissions for banking; number two for rail signaling systems and military radio communications and number three for avionics, civil satellites and surface radars.

The company's 67,000 employees are divided into six global business units that address mixed military and civil markets. Theses business units are:

- Secure Communications and Information Systems
- Land and Air Systems
- Defense Mission Systems
- Avionics
- Space
- Ground Transportation Systems

A.1.2 Thales Avionics

The Avionics global business unit comprises seven business lines, including commercial avionics, military avionics, and helicopter avionics. The avionics business unit employs over 10,000 people and has a leadership position in Europe. It ranks number three in the world behind Honeywell and Rockwell Collins. The military market accounts for 30% of the avionics business.

Thales Avionics offers integrated and modular avionics systems, comprising sensors, actuators and calculators. Its services include control laws design and tuning. Thales solutions are fitted on over 5,000

civil and para-public helicopters and 2,000 military helicopters worldwide. Manufacturers include Agusta Westland, Bell Helicopter, Boeing, Eurocopter, Sikorsky and other majors.

The helicopter offer includes:

- Integrated avionics suite
- GPS and GNSS solutions
- ADU solutions
- HTAWS solutions
- Integrated helmets
- Etc.

A.1.3 The PGV department

The internship takes place within the flight Guidance Product Department ("PGV" that stands for "Produits de Guidage du Vol"). The department consists of 3 differentiated teams: "System Engineering service", "Software service" and "Control Law service". More precisely, this internship will be developed within the "Flight Control Laws service". The "Control Laws service" is in charge of the design and architecture of the control laws for the autopilot functions. A control law is a function of the autopilot that allows control of various aircraft parameters, depending on the selected mode of operation (altitude, trajectory, speed).